Non-classical correlations of scattered photons in a one-dimensional waveguide with multiple two-level emitters

Dibyendu Roy
*Theoretical Division and Center for Nonlinear Studies,
Los Alamos National Laboratory, Los Alamos, New Mexico 87545, USA*

We study the scaling of photon-photon correlations mediated by resonant interactions of photons with two-level emitters in a one-dimensional photonic waveguide. Recently a new theoretical approach based on the Bethe-ansatz technique has been developed to study transport in an open quantum impurity. Here we generalize the approach to study multiple emitters–for example, atoms or quantum dots. We derive the exact solution of single and two-photon scattering states, and the corresponding photon transmission through the emitter ensemble. Correlations of photons at the both ends of the waveguide are examined carefully for one, two and three emitters. We show how various two-photon nonlinear effects, such as spatial attraction and repulsion between photons as well as background fluorescence can be tuned by changing the number of emitters and the coupling between emitters (controlled by the separation). Finally we propose a simple scheme for nonreciprocal optical transmission in the waveguide by placing emitters with different transition energies. Our fully quantum-mechanical approach provides a better understanding of cascaded optical nonlinearity at the microscopic level.

I. INTRODUCTION

Strong coherent photon-photon correlations at the level of few atoms and photons have been demonstrated in various quantum optics set-ups [1–14]. The efficiency of a single or few atoms to induce strong interactions between propagating photons is indispensable to realize various logic gates for quantum information processing, quantum computation and alternative technologies based on switching and amplification functionalities. One interesting recent proposal to achieve strong coherent photon-photon interactions is by confining photons in the reduced dimensions, such as, in a one dimensional (1D) optical waveguide, and coupling these photons with individual emitters in the waveguide [15–24]. Tight confinement of light fields in the waveguide directs the majority of the spontaneously emitted light from the emitter into the transport channels, while local interactions at the emitter induce strong photon-photon correlations by preventing multiple occupancy of photons at the emitter. Various nanoscale systems, such as photonic crystal waveguides [25], surface plasmon modes of metallic nanowires [26], microwave transmission lines [11, 27], optical nanofibers [6, 28], semiconductor or diamond nanowires [29, 30] would act as 1D continuum for photons. Different two- or multi-level atoms [1, 4–6, 10, 28], molecules [9], quantum dots [26, 29], superconducting qubits [5, 11, 27], nitrogen-vacancy centres in diamond [30] are used as an emitter to couple with the 1D continuum of photons.

Recently a nonperturbative fully quantum mechanical approach based on the Bethe-ansatz technique has been developed to study scattering of photons from an emitter in 1D [15, 18, 19]. The main feature of the approach is a proper inclusion of essential open boundary conditions. This is in contrast to the earlier Bethe-ansatz techniques assuming a periodic boundary condition to obtain thermodynamic information of the quantum impurity problems. Several interesting phenomena, such as a two-photon bound state [15], the background fluorescence [15], a single-photon transistor [16], a few-photon diode [18], the scaling of electromagnetically induced transparency with number of photons [19], the stimulated emission [24] have been studied in different systems with a single two-level or three-level emitter coupled to a 1D continuum of photons using the Bethe-ansatz approach. Many of these proposals are already tested in experiments [9, 12, 26]. The Hamiltonian describing the waveguide-emitter system also elucidates the interactions of a light beam with an emitter in three dimension (3D), when the beam is designed to mode-match the emitter's radiation pattern [8, 9, 24, 31, 32]. Therefore, studies using the open Bethe-ansatz method including our results in the present paper should be also relevant to a wide class of recent experiments [9, 12] in 3D.

At this point it is interesting to ask how these phenomena scale with increasing number of emitters in the waveguide. It has been demonstrated that non-classical photon-photon correlations, such as antibunching and sub-Poissonian photon statistics are mostly washed out when more than one atom is excited by low intensity, monochromatic laser light [33, 34]. The quantum statistical characteristics of radiation produced by a cooperative system of two and more emitters in 3D have been studied in detail without [35–38] and with [39–41] including the interactions between emitters. Though we are not aware of any previous study about quantum features of photon-photon correlations for multiple two-level emitters in a 1D waveguide. Here we generalize the open Bethe-ansatz approach to multiple emitters. We calculate the exact single and two-photon scattering states, and the photon transmission through the emitter ensemble. Correlations of photons at the entrance and the exit of the waveguide are examined carefully for one, two and three emitters. We show how different two-photon nonlinear effects, such as spatial attraction and repulsion be-

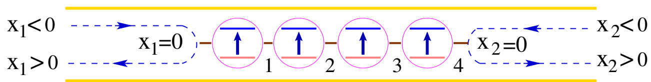

FIG. 1. A schematic of a chain of two-level emitters embedded in a one-dimensional wave-guide, and the propagating free photon modes at the left and the right sides of the emitters.

tween photons as well as background fluorescence can be tuned by changing the number of emitters and the coupling between emitters. The coupling between emitters in the present set-up is determined by the separation between them. Later we show that an emitter ensemble in a 1D waveguide is a suitable model for realizing a fully quantum optical-diode at low light intensity. It is within the reach of present quantum-optics technologies to control the number of emitters in a photonic waveguide with a strong emitter-photon coupling. Our fully quantum-mechanical approach for transport in open systems provides a better understanding of cascaded optical nonlinearity in 1D at the microscopic level.

In Sec.II we outline the open Bethe-ansatz approach in detail for two emitters in a 1D waveguide and propagating photon modes. Single and two-photon dynamics are investigated respectively in Subsec.II A and II B. Nonreciprocal photon transmission for emitters with different transition energies is demonstrated in Subsec.II C. Results of single and two-photon dynamics for three emitters in the waveguide are obtained in two subsections of Sec.III. We conclude with a discussion of our main results and some future directions for further study in Sec.IV.

II. TWO EMITTERS IN A 1D WAVEGUIDE

We consider a chain of two-level emitters coupled to propagating free photons in 1D (see Fig.1). We assume a small separation between emitters for simplicity, thus we can take an instantaneous (vacuum mediated) interaction between emitters. It is so called Markovian limit, where the causal propagation time of photons between two emitters has been neglected [42]. Here we generalize the recently developed Bethe-ansatz approach including open boundary conditions to a chain of multiple emitters coupled to photons. We are able to derive the exact single and two-photon scattering states, and the corresponding photon transmissions in our full system. It is possible to extend our generalized approach to calculate scattering states and transmission for three or more photons. We here give a detailed calculation for a minimal model of the chain, namely a chain of two emitters, and briefly discuss results for a chain of three emitters in the next section. We take the following Hamiltonian to describe the two emitters-photons system. The full Hamiltonian $\mathcal{H} = \mathcal{H}_0 + \mathcal{H}_S + \mathcal{H}_C$ in real space within the rotating-wave approximation for emitter-photon coupling is given by,

$$\begin{aligned}
\mathcal{H}_0 &= -i \int dx\ [v_g^1 \tilde{a}_1^\dagger(x)\partial_x \tilde{a}_1(x) + v_g^2 \tilde{a}_2^\dagger(x)\partial_x \tilde{a}_2(x)],\\
\mathcal{H}_A &= \Omega_1 |2\rangle_{11}\langle 2| + \Omega_2 |2\rangle_{22}\langle 2| + J(\sigma_{1-}\sigma_{2+} + \sigma_{2-}\sigma_{1+}),\\
\mathcal{H}_C &= (\tilde{V}_1 \sigma_{1+}\tilde{a}_1(0) + \tilde{V}_2 \sigma_{2+}\tilde{a}_2(0) + H.c.), \qquad (2.1)
\end{aligned}$$

where the first term $\mathcal{H}_0$ represents the propagating photon modes with group velocity v_g^j at the left ($j = 1$) and the right ($j = 2$) side of the chain; the second term corresponds to the chain of emitters; and the last term describes an interaction between the emitters and the free photons. Here Ω_j is a transition energy of the jth emitter and J is a coupling between the emitters. $\tilde{V}_1$ ($\tilde{V}_2$) is a coupling between the photons at the left (right) side of the chain and the emitters. $\tilde{a}_1^\dagger(x)$ and $\tilde{a}_2^\dagger(x)$ denote creation operators of a photon at the left and the right of the chain respectively. $\sigma_{j-} = c_{jg}^\dagger c_{je}$ ($\sigma_{j+} = c_{je}^\dagger c_{jg}$) is a lowering (raising) ladder operator of the jth emitter where $c_{jg}^\dagger(c_{je}^\dagger)$ is a creation operator of the ground state $|1\rangle_j$ (excited state $|2\rangle_j$) of the jth emitter. Also one can include spontaneous emission from the excited states of the emitters to other photon modes, which are not part of the propagating free photon modes in the above Hamiltonian, by including an imaginary part to the energies of the excited states of the emitters within the quantum-jump approach [19, 43, 44]. Next we scale the free photon operators to absorb the group velocity, and redefine $\sqrt{v_g^j}\tilde{a}_j(x) \equiv a_j(x)$, $\tilde{V}_j/\sqrt{v_g^j} \equiv V_j$. Therefore we rewrite $\mathcal{H}_0 = -i\int dx \sum_{j=1,2} a_j^\dagger(x)\partial_x a_j(x)$ and $\mathcal{H}_C = \sum_{j=1,2} V_j \sigma_{j+} a_j(0) + H.c.$. Hereafter we always consider the transformed Hamiltonian.

A. Single-photon dynamics

First we derive a single-photon scattering state and the corresponding transmission coefficient. We consider that an incident photon with wave-vector k (and energy $E_k = k$) is injected from the left of the emitters. In our approach the wave-function at the left and the right sides of the emitters at $x < 0$ describes the full system before scattering of photons from the emitters, and the wave-function at $x > 0$ characterizes the system after scattering. The single-photon incident state is $|\psi^1_{\rm in}\rangle$, and the wave-function after scattering is $|\psi^1_{\rm out}\rangle$.

$$\begin{aligned}
|\psi^1_{\rm in}\rangle &= \frac{1}{\sqrt{2\pi}} \int dx\ e^{ikx} a_1^\dagger(x)|0,1,1\rangle,\\
|\psi^1_{\rm out}\rangle &= \frac{1}{\sqrt{2\pi}} \int dx \big[(\phi_k^1(x) a_1^\dagger(x) + \phi_k^2(x) a_2^\dagger(x))|0,1,1\rangle\\
&\quad + \delta(x)(e_k^1|0,2,1\rangle + e_k^2|0,1,2\rangle)\big]. \qquad (2.2)
\end{aligned}$$

Here $|n, l_1, m_2\rangle$ denotes state of the full system where n number of photons in the waveguide, left emitter in l_1 state and right emitter in m_2 state. e_k^j is an occupation amplitude of the jth emitter in the excited state. We find

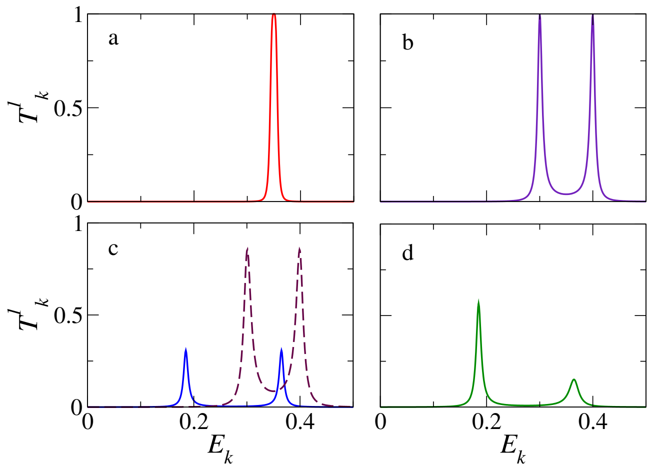

FIG. 2. Single photon transmission T_k^1 through two emitters versus energy E_k of an incident photon. In all plots, $\Omega_2 = 0.35$, $\Gamma_1 = 0.01$ and (a) $\Omega_1 = 0.35$, $\Gamma_2 = 0.01$, $J = 0.005$, (b) $\Omega_1 = 0.35$, $\Gamma_2 = 0.01$, $J = 0.05$, (c) $\Omega_1 = 0.2$, $\Gamma_2 = 0.01$, $J = 0.05$ (blue full curve), $\Omega_1 = 0.35$, $\Gamma_2 = 0.0225$, $J = 0.05$ (maroon dash curve) and (d) $\Omega_1 = 0.2$, $\Gamma_2 = 0.0225$, $J = 0.05$.

different amplitudes in $|\psi^1_{\rm out}\rangle$ by solving the following linear equations obtained from the stationary single-photon Schrödinger equation.

$$-i\partial_x\phi^1_k(x) - E_k\phi^1_k(x) + V_1 e^1_k\delta(x) = 0, \tag{2.3}$$
$$-i\partial_x\phi^2_k(x) - E_k\phi^2_k(x) + V_2 e^2_k\delta(x) = 0, \tag{2.4}$$
$$(\Omega_1 - E_k)e^1_k + V_1\phi^1_k(x)\delta(x) + Je^2_k = 0, \tag{2.5}$$
$$(\Omega_2 - E_k)e^2_k + V_2\phi^2_k(x)\delta(x) + Je^1_k = 0. \tag{2.6}$$

From Eqs.2.3,2.4 we get discontinuity of photon wave-functions across zero, $\phi^1_k(0+) = \phi^1_k(0-) - iV_1e^1_k$,and $\phi^2_k(0+) = \phi^2_k(0-) - iV_2e^2_k$. Using the initial conditions $\phi^1_k(0-) = 1$ and $\phi^2_k(0-) = 0$ for an incident photon from the left, and the regularization across zero, $\phi^i_k(0) = [\phi^i_k(0+) + \phi^i_k(0-)]/2$, we find $\phi^1_k(0) = 1-iV_1e^1_k/2$, $\phi^2_k(0) = -iV_2e^2_k/2$. These results along with Eqs.2.5,2.6 give the amplitudes of excited state,

$$e^2_k = \frac{Je^1_k}{E_k - \Omega_2 + i\Gamma_2/2}, \quad \text{where} \quad \Gamma_i = V_i^2,$$
$$e^1_k = \frac{V_1}{(E_k - \Omega_1 + i\frac{\Gamma_1}{2}) - \frac{J^2}{E_k - \Omega_2 + i\Gamma_2/2}} = \frac{V_1}{\chi + i\frac{\Gamma_1}{2}}. \tag{2.7}$$

Next we calculate the amplitudes of outgoing photon states at the both sides of the emitters.

$$\phi^1_k(x) = e^{ikx}\ \theta(-x) + \frac{\chi - i\Gamma_1/2}{\chi + i\Gamma_1/2}e^{ikx}\ \theta(x),$$
$$\phi^2_k(x) = \frac{-iV_1V_2J}{(\chi + i\Gamma_1/2)(E_k - \Omega_2 + i\Gamma_2/2)}e^{ikx}\theta(x), \tag{2.8}$$

where the single-photon transmission and reflection amplitudes are respectively $t^1_k = \frac{-iV_1V_2J}{(\chi+i\Gamma_1/2)(E_k-\Omega_2+i\Gamma_2/2)}$ and $r^1_k = \frac{\chi-i\Gamma_1/2}{\chi+i\Gamma_1/2}$. For a same value of the left and the right coupling $\Gamma_1 = \Gamma_2 = \Gamma$, and identical emitters $\Omega_1 = \Omega_2 = \Omega$, the transmission coefficient $T^1_k = |t^1_k|^2$ becomes one for $E_k = \Omega$ and $J = \Gamma/2$ (see Fig.2(a)), and the corresponding reflection coefficient is zero. We call it a single peak resonance (SPR). We plot transmission coefficient through two emitters in Fig.2 for different parameter sets. It shows that the transmission curve always has two peaks except for a particular set of parameters shown in Fig.2(a). Also, the single-photon transmission curve becomes asymmetric in shape only when both $\Omega_1 \neq \Omega_2$ and $\Gamma_1 \neq \Gamma_2$. The transmission of a single photon can be detected by analyzing the temporal correlations of photons at the exit of the waveguide using single photon detectors for optical frequencies and linear detectors for microwave frequencies [45].

B. Two-photon dynamics

It is easier to evaluate two-photon scattering state for a single emitter coupled to photons by introducing an even-odd transformation of the photons at the left and the right sides of the emitter. This transformation simplifies the calculation of the scattering state as the transformed even mode of photons is only coupled to the emitter while the transformed odd mode of photons is decoupled from the emitter [15, 18, 19]. Similar transformation of free photon modes is not useful for this problem as different emitters are coupled to photon modes at the left and right sides of the chain. Instead we derive two-photon scattering state directly using photon modes at the left and right sides of the chain. This path will also help us later to derive scattering states for a chain with multiple emitters. The two-photon incoming state $|\psi^2_{\rm in}\rangle$ for both the photons being injected from the left is given by,

$$|\psi^2_{\rm in}\rangle = \int dx_1dx_2\phi_{\mathbf{k}}(x_1,x_2)\frac{1}{\sqrt{2}}a^\dagger_1(x_1)a^\dagger_1(x_2)|0,1,1\rangle, \tag{2.9}$$

where $\phi_{\mathbf{k}}(x_1,x_2) = (e^{ik_1x_1+ik_2x_2} + e^{ik_1x_2+ik_2x_1})/2\pi\sqrt{2}$ with the incident wave vector $\mathbf{k} = (k_1,k_2)$. The total energy of two incident photons $E_{\mathbf{k}} = k_1 + k_2$. We write a general two-photon scattering state $|\psi^2_{\rm out}\rangle$ using the operators of free photon modes and emitters.

$$\begin{aligned}|\psi^2_{\rm out}\rangle = \int dx_1dx_2\Big[&\{g_{11}(x_1,x_2)\frac{1}{\sqrt{2}}a^\dagger_1(x_1)a^\dagger_1(x_2)\\ &+e^1_1(x_1)\delta(x_2)a^\dagger_1(x_1)\sigma_{1+} + e^2_1(x_1)\delta(x_2)a^\dagger_1(x_1)\sigma_{2+}\\ &+e_{12}\delta(x_1)\delta(x_2)\sigma_{1+}\sigma_{2+}\} + \{g_{12}(x_1;x_2)a^\dagger_1(x_1)a^\dagger_2(x_2)\\ &+e^1_2(x_1)\delta(x_2)a^\dagger_2(x_1)\sigma_{1+} + e^2_2(x_1)\delta(x_2)a^\dagger_2(x_1)\sigma_{2+}\}\\ &+g_{22}(x_1,x_2)\frac{1}{\sqrt{2}}a^\dagger_2(x_1)a^\dagger_2(x_2)\Big]|0,1,1\rangle,\end{aligned} \tag{2.10}$$

where $g_{11}(x_1,x_2) \equiv g_{11}(x_2,x_1)$ and $g_{22}(x_1,x_2) \equiv g_{22}(x_2,x_1)$ for the Bose statistics of photons. The ampli-

tudes $g_{11}(x_1,x_2)$, $g_{22}(x_1,x_2)$, and $g_{12}(x_1;x_2)$ denote outgoing two-photon wave-functions, in which either both photons are transmitted or reflected, or one photon is transmitted while the other is reflected. A simple thought experimental set-up has been proposed in Ref.[15] to measure the magnitude of these wave-functions. In this set-up, a beam splitter with a single-photon counter on each of the output arm of the beam splitter, is placed at the entrance and the exit of the 1D photonic waveguide. The measurement of the wave-functions are carried out by varying the distance of the photo-detectors after injecting a weak classical beam with the average photon numbers per pulse being much lower than two, and the pulse repetition rate being much smaller than the spontaneous emission rate of the emitters. Here $e_1^1(x), e_1^2(x)$ $(e_2^1(x), e_2^2(x))$ are the probability amplitudes of one photon in the left (right) side of the emitters while respectively the left or the right emitter is in the excited state. Also, e_{12} is the probability amplitude of both the emitters are in excited state. We determine all the amplitudes in Eq.(2.10) using the two-photon Schrödinger equation. Thus, we obtain the following set of linear coupled first order differential equations.

$$\Big(-i(\partial_{x_1}+\partial_{x_2})-E_{\mathbf{k}}\Big)g_{11}(x_1,x_2)+\frac{V_1}{\sqrt{2}}[e_1^1(x_1)\delta(x_2)+\delta(x_1)e_1^1(x_2)]=0, \tag{2.11}$$

$$\Big(-i\partial_x-E_{\mathbf{k}}+\Omega_1\Big)e_1^1(x)+\frac{V_1}{\sqrt{2}}[g_{11}(0,x)+g_{11}(x,0)]+Je_1^2(x)=0, \tag{2.12}$$

$$\Big(-i\partial_x-E_{\mathbf{k}}+\Omega_2\Big)e_1^2(x)+V_2g_{12}(x;0)+Je_1^1(x)+V_1e_{12}\delta(x)=0, \tag{2.13}$$

$$(\Omega_1+\Omega_2-E_{\mathbf{k}})e_{12}+V_1e_1^2(0)+V_2e_2^1(0)=0, \tag{2.14}$$

$$\Big(-i(\partial_{x_1}+\partial_{x_2})-E_{\mathbf{k}}\Big)g_{22}(x_1,x_2)+\frac{V_2}{\sqrt{2}}[e_2^2(x_1)\delta(x_2)+\delta(x_1)e_2^2(x_2)]=0, \tag{2.15}$$

$$\Big(-i\partial_x-E_{\mathbf{k}}+\Omega_1\Big)e_2^1(x)+V_1g_{12}(0;x)+Je_2^2(x)+V_2e_{12}\delta(x)=0, \tag{2.16}$$

$$\Big(-i\partial_x-E_{\mathbf{k}}+\Omega_2\Big)e_2^2(x)+\sqrt{2}V_2g_{22}(0,x)+Je_2^1(x)=0, \tag{2.17}$$

$$\Big(-i(\partial_{x_1}+\partial_{x_2})-E_{\mathbf{k}}\Big)g_{12}(x_1;x_2)+V_2e_1^2(x_1)\delta(x_2)+V_1\delta(x_1)e_2^1(x_2)=0. \tag{2.18}$$

The initial conditions for the amplitudes are chosen such that $g_{11}(x_1,x_2)$, $g_{22}(x_1,x_2)$, and $g_{12}(x_1;x_2)$ at the region $x_1,x_2<0$ correspond to plane wave-function of the Eq.(2.9). Thus, for both the photons being injected from the left, $g_{11}(x_1<0,x_2<0)=\phi_{\mathbf{k}}(x_1,x_2)$, $g_{22}(x_1<0,x_2<0)=0$, $g_{12}(x_1<0;x_2<0)=0$. We use the following regularization of these amplitudes across $x_1,x_2=0$ as $g_{11}(0,x)\equiv g_{11}(x,0)=[g_{11}(0+,x)+g_{11}(0-,x)]/2$, $g_{22}(0,x)\equiv g_{22}(x,0)=[g_{22}(0+,x)+g_{22}(0-,x)]/2$, $g_{12}(0;x)=[g_{12}(0+;x)+g_{12}(0-;x)]/2$ and $g_{12}(x;0)=[g_{12}(x;0+)+g_{12}(x;0-)]/2$.

From Eqs.(2.11,2.15,2.18) we get the discontinuity relations of the two-photon amplitudes across zero, $g_{jj}(x_1,0+)=g_{jj}(x_1,0-)-iV_je_j^j(x_1)/\sqrt{2}$, $g_{jj}(0+,x_2)=g_{jj}(0-,x_2)-iV_je_j^j(x_2)/\sqrt{2}$, for $j=1,2$, $g_{12}(x_1;0+)=g_{12}(x_1;0-)-iV_2e_1^2(x_1)$, $g_{12}(0+;x_2)=g_{12}(0-;x_2)-iV_1e_2^1(x_2)$. We also find the discontinuity relations of the emitter-photon amplitudes from Eqs.(2.12,2.13,2.16,2.17), $e_1^1(0+)=e_1^1(0-)$, $e_1^2(0+)=e_1^2(0-)-iV_1e_{12}$, $e_2^1(0+)=e_2^1(0-)-iV_2e_{12}$, $e_2^2(0+)=e_2^2(0-)$. Next we determine e_{12} from Eq.(2.14) and the previous relations for $e_1^2(0)$ and $e_2^1(0)$. We find

$$e_{12}=-\frac{V_1e_1^2(0-)+V_2e_2^1(0-)}{\Omega_1+\Omega_2-E_{\mathbf{k}}-i(\Gamma_1+\Gamma_2)/2}. \tag{2.19}$$

Now we derive the amplitudes of an excited emitter explicitly. We rewrite the coupled linear inhomogeneous first-order differential equations in Eqs.2.12,2.13 in a matrix notation; we find

$$-i\partial_x\begin{pmatrix}e_1^1(x)\\ e_1^2(x)\end{pmatrix}=\begin{pmatrix}E_{\mathbf{k}}-\Omega_1+iV_1^2/2 & -J\\ -J & E_{\mathbf{k}}-\Omega_2+iV_2^2/2\end{pmatrix}\begin{pmatrix}e_1^1(x)\\ e_1^2(x)\end{pmatrix}-\begin{pmatrix}\sqrt{2}V_1g_{11}(x,0-)\\ V_2g_{12}(x;0-)\end{pmatrix}-\begin{pmatrix}0\\ V_1e_{12}\end{pmatrix}\delta(x). \tag{2.20}$$

The eigenvalues of the above 2×2 square matrix (call $\overleftrightarrow{\mathbf{A}}$) are $\lambda_\pm=E_{\mathbf{k}}-(\Omega_1+\Omega_2)/2+i(\Gamma_1+\Gamma_2)/4\pm\beta/4$ where $\beta=\sqrt{\alpha^2+16J^2}$ and $\alpha=2(\Omega_2-\Omega_1)+i(\Gamma_1-\Gamma_2)$. The inverse of the 2×2 square matrix $\overleftrightarrow{\mathbf{P}}[\equiv(|\lambda_-\rangle,|\lambda_+\rangle)]$ formed with

the eigenvectors $|\lambda_-\rangle$ and $|\lambda_+\rangle$ of $\overleftrightarrow{\mathbf{A}}$ in Eq.2.20 is

$$\overleftrightarrow{\mathbf{P}}^{-1} = \begin{pmatrix} \frac{2J}{\beta} & \frac{\alpha+\beta}{2\beta} \\ -\frac{2J}{\beta} & \frac{-\alpha+\beta}{2\beta} \end{pmatrix} \text{ and } \overleftrightarrow{\mathbf{P}}^{-1}\overleftrightarrow{\mathbf{A}}\overleftrightarrow{\mathbf{P}} = \begin{pmatrix} \lambda_- & 0 \\ 0 & \lambda_+ \end{pmatrix}.$$

Therefore, we can write the coupled equations in Eq.2.20 in a rotated frame using the transformed excitation amplitudes of the emitters, $\tilde{e}_1^1(x) = \frac{2J}{\beta}e_1^1(x) + \frac{\alpha+\beta}{2\beta}e_1^2(x)$, $\tilde{e}_1^2(x) = -\frac{2J}{\beta}e_1^1(x) + \frac{-\alpha+\beta}{2\beta}e_1^2(x)$, and the inverse transformations are $e_1^2(x) = \tilde{e}_1^1(x) + \tilde{e}_1^2(x)$ and $e_1^1(x) = \frac{\beta}{2J}(\frac{1}{2} - \frac{\alpha}{2\beta})\tilde{e}_1^1(x) - \frac{\beta}{2J}(\frac{1}{2} + \frac{\alpha}{2\beta})\tilde{e}_1^2(x)$. The transformed matrix equation,

$$\partial_x \begin{pmatrix} \tilde{e}_1^1(x) \\ \tilde{e}_1^2(x) \end{pmatrix} = i \begin{pmatrix} \lambda_- & 0 \\ 0 & \lambda_+ \end{pmatrix} \begin{pmatrix} \tilde{e}_1^1(x) \\ \tilde{e}_1^2(x) \end{pmatrix} - \overleftrightarrow{\mathbf{P}}^{-1} i \begin{pmatrix} \sqrt{2}V_1 g_{11}(x,0-) \\ V_2 g_{12}(x;0-) \end{pmatrix} - \overleftrightarrow{\mathbf{P}}^{-1} i \begin{pmatrix} 0 \\ V_1 e_{12} \end{pmatrix} \delta(x). \quad (2.21)$$

We find the following discontinuity relations across zero for the transformed amplitudes from Eq.2.21, $\tilde{e}_1^1(0+) = \tilde{e}_1^1(0-) - i\frac{\alpha+\beta}{2\beta}V_1 e_{12}$, $\tilde{e}_1^2(0+) = \tilde{e}_1^2(0-) - i\frac{-\alpha+\beta}{2\beta}V_1 e_{12}$.

For the incident photons coming from the left $g_{12}(x;0-) = 0$ at any x; we use the incident condition of $g_{11}(x < 0, 0-)$ and find $\tilde{e}_1^1(x)$ and $\tilde{e}_1^2(x)$ at $x < 0$ from the Eqs.2.21

$$\tilde{e}_1^1(x<0) = \frac{J}{\pi\beta}(\varepsilon_{k_1}e^{ik_2x} + \varepsilon_{k_2}e^{ik_1x}), \quad \text{where}$$
$$\varepsilon_k = \frac{V_1}{k - (\Omega_1+\Omega_2)/2 + i(\Gamma_1+\Gamma_2)/4 - \beta/4},$$
$$\tilde{e}_1^2(x<0) = -\frac{J}{\pi\beta}(\varsigma_{k_1}e^{ik_2x} + \varsigma_{k_2}e^{ik_1x}), \quad \text{where}$$
$$\varsigma_k = \frac{V_1}{k - (\Omega_1+\Omega_2)/2 + i(\Gamma_1+\Gamma_2)/4 + \beta/4}.$$

We now get back the original amplitudes for emitters' excitation using the inverse transformations.

$$e_1^1(x<0) = \frac{1}{2\pi}(e_{k_1}^1 e^{ik_2x} + e_{k_2}^1 e^{ik_1x}),$$
$$e_1^2(x<0) = \frac{1}{2\pi}(e_{k_1}^2 e^{ik_2x} + e_{k_2}^2 e^{ik_1x}). \quad (2.22)$$

Physically these amplitudes describe part of the wavefunction in which one photon is at $x < 0$ of the incident photon channel while the other photon is absorbed by an emitter to reach to an excited state. The expressions in Eq.2.22 clearly reflect it. Similarly we rewrite Eqs.(2.16,2.17) in a matrix notation, and then transform it by multiplying $\overleftrightarrow{\mathbf{P}}^{-1}$ from the left. Thus we find

$$\partial_x \begin{pmatrix} \tilde{e}_2^1(x) \\ \tilde{e}_2^2(x) \end{pmatrix} = i \begin{pmatrix} \lambda_- & 0 \\ 0 & \lambda_+ \end{pmatrix} \begin{pmatrix} \tilde{e}_2^1(x) \\ \tilde{e}_2^2(x) \end{pmatrix} - \overleftrightarrow{\mathbf{P}}^{-1} i \begin{pmatrix} V_1 g_{12}(0-;x) \\ \sqrt{2}V_2 g_{22}(0-,x) \end{pmatrix} - \overleftrightarrow{\mathbf{P}}^{-1} i \begin{pmatrix} V_1 e_{12} \\ 0 \end{pmatrix} \delta(x), \quad (2.23)$$

where $\tilde{e}_2^1(x) = \frac{2J}{\beta}e_2^1(x) + \frac{\alpha+\beta}{2\beta}e_2^2(x)$, $\tilde{e}_2^2(x) = -\frac{2J}{\beta}e_2^1(x) + \frac{-\alpha+\beta}{2\beta}e_2^2(x)$. As, $g_{22}(0-,x), g_{12}(0-;x) = 0$ for $x < 0$, we find $\tilde{e}_2^1(x<0) = 0$ and $\tilde{e}_2^2(x<0) = 0$. Therefore, $e_2^1(x<0) = e_2^2(x<0) = 0$, i.e., the amplitude of one of the emitters being excited while one photon at $x < 0$ at the right side of the emitters is zero. It is physically acceptable, the causality prevents an injected photon from the left to move at $x < 0$ of the right side photon channel. We now determine e_{12}, $g_{11}(x, 0+)$, $g_{11}(0+, x)$, $g_{22}(x, 0+)$, $g_{22}(0+, x)$, $g_{12}(x; 0+)$, and $g_{12}(0+; x)$ at $x < 0$ from the amplitudes of an excited emitter. We find explicit expression for the amplitude e_{12} from Eq.2.19 by inserting $e_1^2(0-)$ and $e_2^1(0-)$.

$$e_{12} = \frac{iV_1}{2\pi V_2}\frac{t_{k_1}^1 + t_{k_2}^1}{E_{\mathbf{k}} - \Omega_1 - \Omega_2 + \frac{i}{2}(\Gamma_1+\Gamma_2)}, \quad (2.24)$$

which shows that e_{12} is non-zero only when a single photon transmission amplitude is non-zero at least for one incident photon energy. The amplitude of one photon being reflected while the other photon is still at the incident side is given by

$$g_{11}(x_1<0, x_2>0) = g_{11}(x_2>0, x_1<0)$$
$$= \frac{1}{2\sqrt{2}\pi}(r_{k_1}^1 e^{ik_2x_1+ik_1x_2} + r_{k_2}^1 e^{ik_1x_1+ik_2x_2}). \quad (2.25)$$

Similarly we find the two-photon amplitudes, $g_{22}(x_1 < 0, x_2 > 0) = g_{22}(x_2 > 0, x_1 < 0) = 0$, $g_{12}(x_1 > 0; x_2 < 0) = 0$, and the amplitude of only one photon being transmitted while the other being at the incident channel is

$$g_{12}(x_1<0; x_2>0)$$
$$= \frac{1}{2\pi}(e^{ik_1x_1+ik_2x_2}t_{k_2}^1 + e^{ik_1x_2+ik_2x_1}t_{k_1}^1)). \quad (2.26)$$

Next we calculate $\tilde{e}_1^1(x)$, $\tilde{e}_1^2(x)$, $\tilde{e}_2^1(x)$ and $\tilde{e}_2^2(x)$ at $x > 0$ from Eqs.2.21,2.23 using $g_{11}(x_1 < 0, x_2 > 0)$, $g_{22}(x_1 <$

$0, x_2 > 0)$ and $g_{12}(x_1 < 0; x_2 > 0)$. We find

$$\tilde{e}_1^1(x>0) = c_1 e^{i\lambda_- x} + \frac{J}{\pi\beta}(r^1_{k_1}\varepsilon_{k_2}e^{ik_1x} + r^1_{k_2}\varepsilon_{k_1}e^{ik_2x}),$$
$$\tilde{e}_1^2(x>0) = c_2 e^{i\lambda_+ x} - \frac{J}{\pi\beta}(r^1_{k_1}\varsigma_{k_2}e^{ik_1x} + r^1_{k_2}\varsigma_{k_1}e^{ik_2x}),$$

where c_1 and c_2 are two constants which we find using discontinuity relations of $\tilde{e}_1^1(x)$ and $\tilde{e}_1^2(x)$ across $x=0$.

$$c_1 = \frac{J}{\pi\beta}((1-r_{k_1})\varepsilon_{k_2} + (1-r_{k_2})\varepsilon_{k_1}) - i\frac{\alpha+\beta}{2\beta}V_1 e_{12},$$
$$c_2 = -\frac{J}{\pi\beta}((1-r_{k_1})\varsigma_{k_2} + (1-r_{k_2})\varsigma_{k_1}) - i\frac{-\alpha+\beta}{2\beta}V_1 e_{12}.$$

The general forms of $e_1^1(x)$ and $e_1^2(x)$ for any value of x are

$$\begin{aligned} e_1^1(x) &= \big(\frac{\beta}{2J}(\frac{1}{2} - \frac{\alpha}{2\beta})c_1 e^{i\lambda_- x} - \frac{\beta}{2J}(\frac{1}{2} + \frac{\alpha}{2\beta})c_2 e^{i\lambda_+ x}\big)\theta(x) \\ &\quad + \frac{1}{2\pi}(e^1_{k_1}\phi^1_{k_2}(x) + e^1_{k_2}\phi^1_{k_1}(x)), \\ e_1^2(x) &= \big(c_1 e^{i\lambda_- x} + c_2 e^{i\lambda_+ x}\big)\theta(x) \\ &\quad + \frac{1}{2\pi}(e^2_{k_1}\phi^1_{k_2}(x) + e^2_{k_2}\phi^1_{k_1}(x)). \end{aligned} \tag{2.27}$$

The first terms in $e_1^1(x)$ and $e_1^2(x)$ are contributions from a two-photon bound state. Similarly we calculate $\tilde{e}_2^1(x), \tilde{e}_2^2(x)$ for $x>0$ from Eq.2.23 using $g_{12}(0-; x>0)$ from Eq.2.26 and $g_{22}(0-, x) = 0$. We get

$$\begin{aligned} \tilde{e}_2^1(x>0) &= \tilde{c}_1 e^{i\lambda_- x} + \frac{J}{\pi\beta}(t^1_{k_1}\varepsilon_{k_2}e^{ik_1x} + t^1_{k_2}\varepsilon_{k_1}e^{ik_2x}), \\ \tilde{e}_2^2(x>0) &= \tilde{c}_2 e^{i\lambda_+ x} - \frac{J}{\pi\beta}(t^1_{k_1}\varsigma_{k_2}e^{ik_1x} + t^1_{k_2}\varsigma_{k_1}e^{ik_2x}), \end{aligned} \tag{2.28}$$

where the constants $\tilde{c}_1$ and $\tilde{c}_2$ are determined using discontinuity relations of $\tilde{e}_2^1(x)$ and $\tilde{e}_2^2(x)$ across zero.

$$\begin{aligned} \tilde{c}_1 &= -\frac{J}{\pi\beta}(t^1_{k_1}\varepsilon_{k_2} + t^1_{k_2}\varepsilon_{k_1}) - \frac{2iJ}{\beta}V_2 e_{12}, \\ \tilde{c}_2 &= \frac{J}{\pi\beta}(t^1_{k_1}\varsigma_{k_2} + t^1_{k_2}\varsigma_{k_1}) + \frac{2iJ}{\beta}V_2 e_{12}. \end{aligned} \tag{2.29}$$

One can find $e_2^1(x),\ e_2^2(x)$ at any x from $\tilde{e}_2^1(x),\ \tilde{e}_2^2(x)$.

$$\begin{aligned} e_2^1(x) &= \big(\frac{\beta}{2J}(\frac{1}{2} - \frac{\alpha}{2\beta})\tilde{c}_1 e^{i\lambda_- x} - \frac{\beta}{2J}(\frac{1}{2} + \frac{\alpha}{2\beta})\tilde{c}_2 e^{i\lambda_+ x}\big)\theta(x) \\ &\quad + \frac{1}{2\pi}(e^1_{k_1}\phi^2_{k_2}(x) + e^1_{k_2}\phi^2_{k_1}(x)), \\ e_2^2(x) &= \big(\tilde{c}_1 e^{i\lambda_- x} + \tilde{c}_2 e^{i\lambda_+ x}\big)\theta(x) \\ &\quad + \frac{1}{2\pi}(e^2_{k_1}\phi^2_{k_2}(x) + e^2_{k_2}\phi^2_{k_1}(x)). \end{aligned} \tag{2.30}$$

We are now ready to evaluate $g_{11}(x_1, x_2)$, $g_{22}(x_1, x_2)$, $g_{12}(x_1; x_2)$ for all values of x_1, x_2. Here we introduce a central of motion coordinate of photons $x_c = (x_1 + x_2)/2$ and a relative motion coordinate $x = (x_1 - x_2)$. The general form of the two-photon amplitudes at different sides of the emitters are

$$\begin{aligned} g_{11}(x_1, x_2) &= \frac{1}{2\pi\sqrt{2}}(\phi^1_{k_1}(x_1)\phi^1_{k_2}(x_2) + \phi^1_{k_2}(x_1)\phi^1_{k_1}(x_2)) - \frac{iV_1\beta}{2\sqrt{2}J}(\frac{1}{2} - \frac{\alpha}{2\beta})c_1 e^{iE_{\mathbf{k}}x_c}e^{i(\lambda_- - E_{\mathbf{k}}/2)|x|}\theta(x_1)\theta(x_2) \\ &\quad + \frac{iV_1\beta}{2\sqrt{2}J}(\frac{1}{2} + \frac{\alpha}{2\beta})c_2 e^{iE_{\mathbf{k}}x_c}e^{i(\lambda_+ - E_{\mathbf{k}}/2)|x|}\theta(x_1)\theta(x_2), \\ g_{22}(x_1, x_2) &= \frac{1}{2\pi\sqrt{2}}(\phi^2_{k_1}(x_1)\phi^2_{k_2}(x_2) + \phi^2_{k_2}(x_1)\phi^2_{k_1}(x_2)) - \frac{iV_2}{\sqrt{2}}(\tilde{c}_1 e^{iE_{\mathbf{k}}x_c}e^{i(\lambda_- - E_{\mathbf{k}}/2)|x|} + \tilde{c}_2 e^{iE_{\mathbf{k}}x_c}e^{i(\lambda_+ - E_{\mathbf{k}}/2)|x|})\theta(x_1)\theta(x_2), \\ g_{12}(x_1; x_2) &= \frac{1}{2\pi}(\phi^1_{k_1}(x_1)\phi^2_{k_2}(x_2) + \phi^1_{k_2}(x_1)\phi^2_{k_1}(x_2)) - iV_1\big(\frac{\beta-\alpha}{4J}\tilde{c}_1 e^{i\lambda_- x_2}e^{i(E_{\mathbf{k}}-\lambda_-)x_1} - \frac{\alpha+\beta}{4J}\tilde{c}_2 e^{i\lambda_+ x_2} \\ &\quad \times e^{i(E_{\mathbf{k}}-\lambda_+)x_1}\big)\theta(x_2 - x_1)\theta(x_1) - iV_2\big(c_1 e^{i\lambda_- x_1}e^{i(E_{\mathbf{k}}-\lambda_-)x_2} + c_2 e^{i\lambda_+ x_1}e^{i(E_{\mathbf{k}}-\lambda_+)x_2}\big)\theta(x_1 - x_2)\theta(x_2). \end{aligned} \tag{2.31}$$

The second terms in $g_{11}(x_1, x_2)$, $g_{22}(x_1, x_2)$ and $g_{12}(x_1; x_2)$ are contributions from a two-photon bound state which arises due to coherent photon-photon interactions mediated by the emitters. We refer them as bound state as these terms fall rapidly with increasing $|x_1 - x_2|$ or $|x|$. Two photons can exchange energy and momentum between themselves after scattering from the emitters due to resonant interactions at the localized region of the emitters. Though the total energy and momentum of the two incident photons remain the same after scattering. This energy-momentum distribution of photons is also the origin of background fluorescence which can be conceived as an inelastic scattering of one photon from a composite transient object formed by the emitter absorbing the other photon. The strength of background fluorescence, i.e., inelastic scattering is much enhanced for the present system in a confined geometry compared to free space in 3D [46]. Here we define a total energy

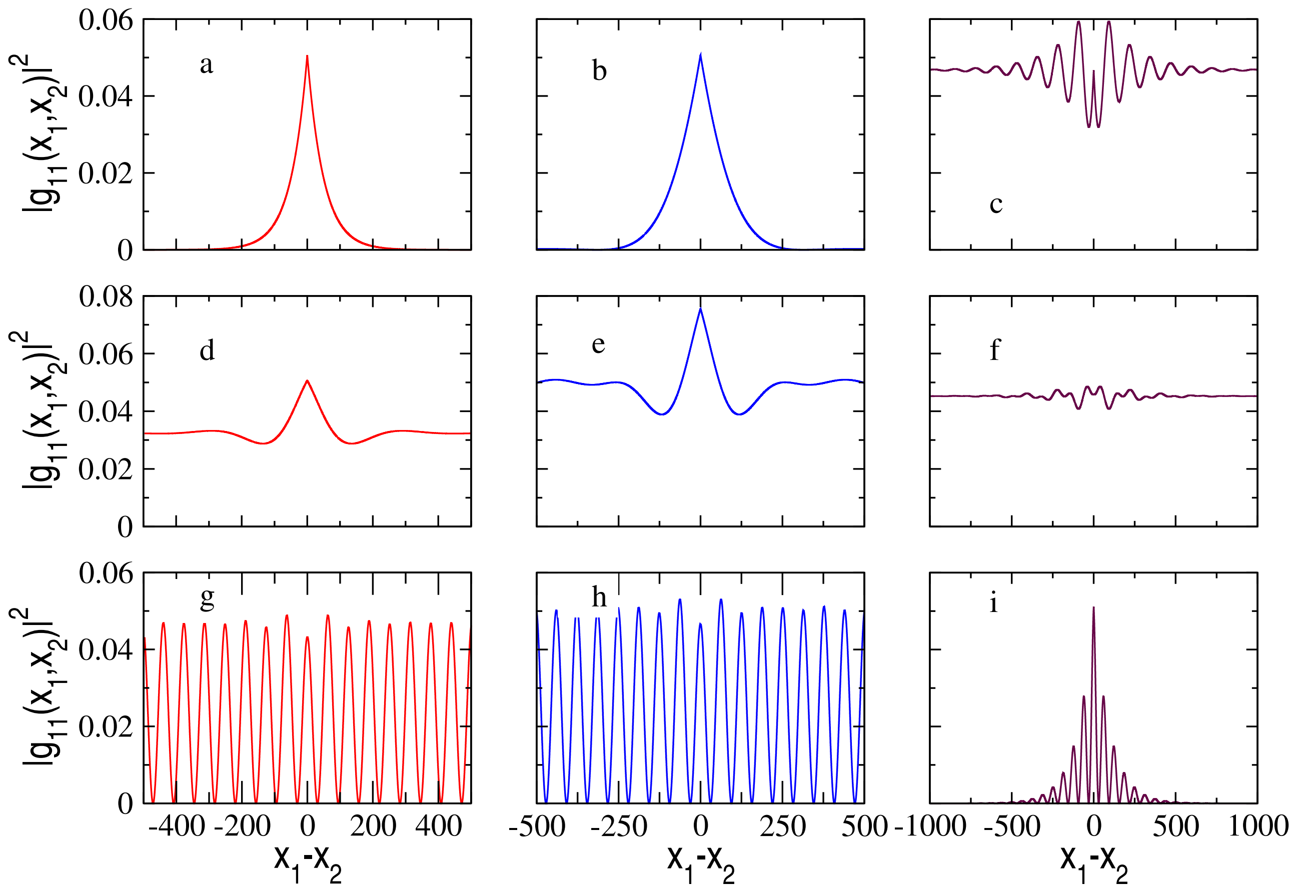

FIG. 3. Two reflected photons wave-function $|g_{11}(x_1, x_2)|^2$ for one emitter (first column) and two emitters (middle and last columns) at various incident photon-pair energy detuning δE and energy difference Δ. We use $\Omega_1 = \Omega_2 = \Omega$ and $\Gamma_1 = \Gamma_2 = \Gamma$ in all the plots for two emitters. The parameters are, (I) Top row: $\delta E = \Delta = 0,\ E_{k_1} = E_{k_2} = \Omega = 0.35,\ \Gamma = 0.01$, (II) Middle row: $\delta E = 0.04,\ \Delta = 0,\ E_{k_1} = E_{k_2} = 0.35,\ \Omega = 0.33,\ \Gamma = 0.01$, and (III) Bottom row: $\delta E = 0,\ \Delta = -0.1,\ E_{k_1} = 0.3,\ E_{k_2} = 0.4,\ \Omega = 0.35,\ \Gamma = 0.01$. The coupling $J = 0.005$ for the middle column and $J = 0.05$ for the last column.

detuning $\delta E \equiv E_{\mathbf{k}} - (\Omega_1 + \Omega_2)$ and a energy difference $\Delta \equiv E_{k_1} - E_{k_2}$. We discuss thoroughly various properties of the outgoing wave-functions by tuning δE and Δ, and compare these results with those for a single emitter in a waveguide.

First we consider form of these wave-functions at single photon resonance of the identical emitters for a same value of the left and the right couplings, i.e., $E_{k_1} = E_{k_2} = \Omega_1 = \Omega_2$ and $V_1 = V_2$. Around these parameter sets, the single photon transmission curve has a single peak for $J = \Gamma/2$ (check Fig.2(a)). The wave-functions at this special point behave as

$$\begin{aligned} g_{11}(x_1, x_2) &= -\frac{1}{\sqrt{2}\pi} e^{iE_{\mathbf{k}}x_c} e^{-\Gamma|x|/2} \cos(\Gamma|x|/2), \\ g_{22}(x_1, x_2) &= -\frac{1}{\sqrt{2}\pi} e^{iE_{\mathbf{k}}x_c} (1 - e^{-\Gamma|x|/2} \cos(\Gamma|x|/2)), \\ g_{12}(x_1, x_2) &= \frac{i}{\pi} e^{iE_{\mathbf{k}}x_c} e^{-\Gamma|x|/2} \sin(\Gamma x/2). \end{aligned} \tag{2.32}$$

These functions for a direct coupled two-level emitter-photons system in a 1D waveguide are $\bar{g}_{11}(x_1, x_2) = -e^{iE_{\mathbf{k}}x_c} e^{-\Gamma|x|/2}/(\sqrt{2}\pi)$, $\bar{g}_{22}(x_1, x_2) = -e^{iE_{\mathbf{k}}x_c}(1 - e^{-\Gamma|x|/2})/(\sqrt{2}\pi)$, $\bar{g}_{12}(x_1; x_2) = -e^{iE_{\mathbf{k}}x_c} e^{-\Gamma|x|/2}/\pi$. Notice that the form of the two-photon wave-functions here for a single emitter at resonance is different from that of the side-coupled emitter studied by Shen and Fan [15]. It is because Shen and Fan consider opposite signs for the group velocity of the left and the right moving propagating photon modes in the side-coupled model. In fact one will get back the results of Shen and Fan (within an overall minus sign for $\bar{g}_{22}(x_1, x_2)$) by changing $x_1 \to -x_1,\ x_2 \to -x_2$ in our results for $\bar{g}_{22}(x_1, x_2)$, and $x_2 \to -x_2$ in our results for $\bar{g}_{12}(x_1, x_2)$. Comparing two-photon wave-functions of a single and two emitters, we find that for the two emitters there is an extra sinusoidal oscillation to the exponentially decaying two reflected photon wave-function of a single direct coupled emitter. This interesting feature shows up because of our instaneous coupling between two emitters which is a valid approximation for small separation between emitters. A similar feature also persists in the two transmitted, and one transmitted-one reflected photons wave-functions. Though, when $|x|$ is small, $|g_{11}(x_1, x_2)|^2$ and

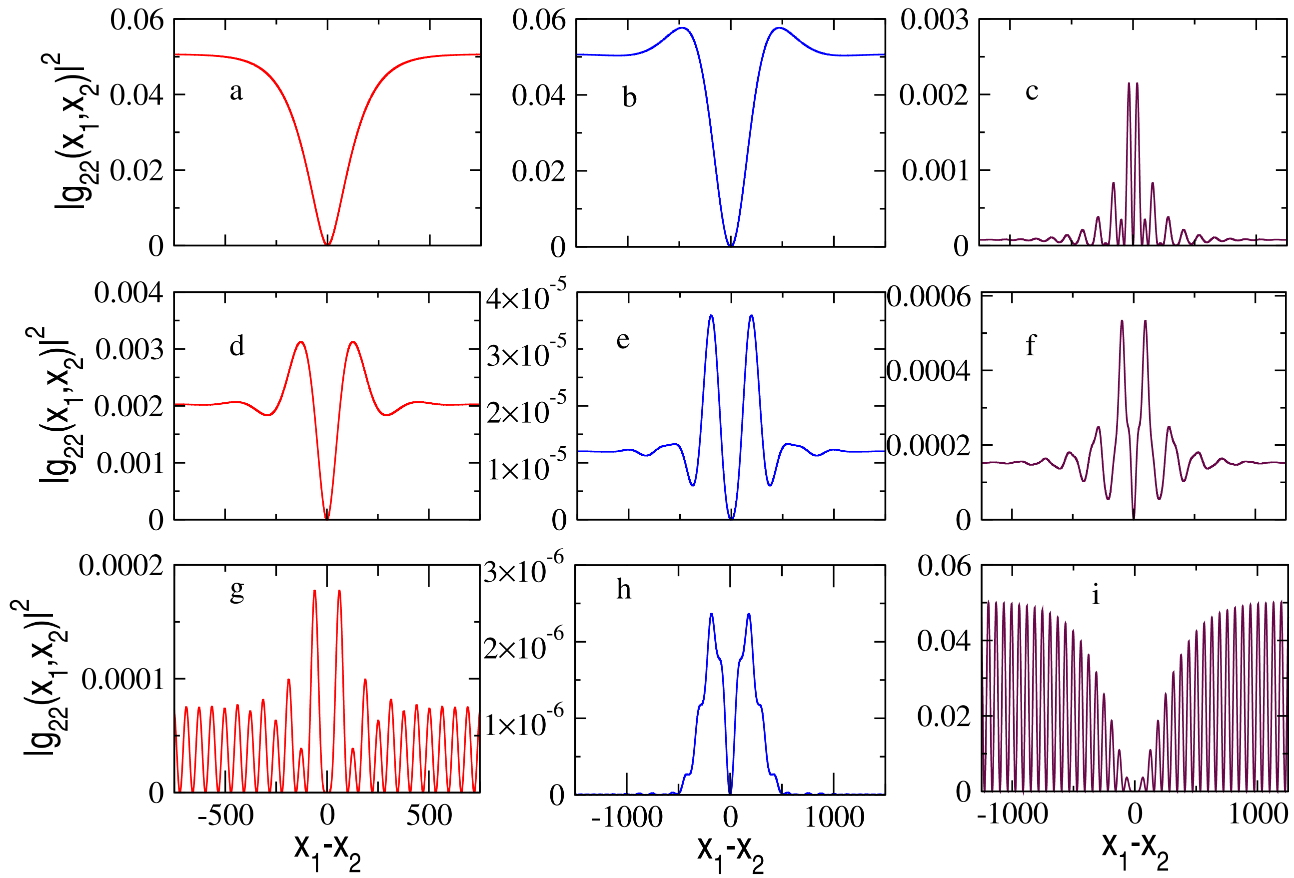

FIG. 4. Two transmitted photons wave-function $|g_{22}(x_1,x_2)|^2$ for one emitter (first column) and two emitters (middle and last columns) at various incident photon-pair energy detuning δE and energy difference Δ. We use $\Omega_1 = \Omega_2 = \Omega$ and $\Gamma_1 = \Gamma_2 = \Gamma$ in all the plots for two emitters. The parameters are, (I) Top row: $\delta E = \Delta = 0,\ E_{k_1} = E_{k_2} = \Omega = 0.35,\ \Gamma = 0.01$, (II) Middle row: $\delta E = 0.04,\ \Delta = 0,\ E_{k_1} = E_{k_2} = 0.35,\ \Omega = 0.33,\ \Gamma = 0.01$, and (III) Bottom row: $\delta E = 0,\ \Delta = -0.1,\ E_{k_1} = 0.3,\ E_{k_2} = 0.4,\ \Omega = 0.35,\ \Gamma = 0.01$. The coupling $J = 0.005$ for the middle column and $J = 0.05$ for the last column.

$|g_{22}(x_1,x_2)|^2$ have similar features for a single and two emitters in a 1D waveguide. The slow sinusoidal oscillations along with a decay of wave-function with increasing distance separation $|x|$ should manifest in the coherence measurement, such as, a measurement of the $g^{(2)}(\tau)$ function in each case [15, 33, 45, 47]. Interestingly it has been shown recently that a normalized second-order correlation of stationary pulse intensity of a strongly interacting photon gas contains a cosine oscillating part which has been indicated as the Friedel oscillations characterizing a strongly interacting gas [48]. We plot $|g_{11}(x_1,x_2)|^2$ for a single and two emitters at single photon resonance in Figs.3(a),(b), and $|g_{22}(x_1,x_2)|^2$ for a single and two emitters at single photon resonance in Figs.4(a),(b). The oscillation due to the cosine term for two emitters is evident in Fig.4(b), and the corresponding curve for a single emitter has no oscillation. Though the oscillation for two emitters in the two reflected photons curve is not quite clear. $|g_{12}(x_1,x_2)|^2$ is shown in Fig.5(a),(b) for a single and two emitters at single photon resonance. The sinusoidal oscillations for two emitters make a sharp change in the pattern of $|g_{12}(x_1,x_2)|^2$ for two emitters compared to a single emitter. While $|g_{12}(x_1,x_2=x_1)|^2$ has a peak of height $1/2\pi^2$ for a single emitter, it is zero for two emitters. Thus, one reflected and one transmitted photons for two emitters are *anti-bunched* at SPR. We show $|g_{11}(x_1,x_2)|^2$, $|g_{22}(x_1,x_2)|^2$ and $|g_{12}(x_1,x_2)|^2$ for two emitters at $J = 0.05$ in Fig.3(c), Fig.4(c) and Fig.5(c) which show a completely different behavior compared to the $J = 0.005$ case for two emitters or a single emitter. There are two peaks in the single photon transmission curve at $J = 0.05$ compared to one peak at $J = 0.005$.

We plot $|g_{11}(x_1,x_2)|^2$ and $|g_{22}(x_1,x_2)|^2$ for a non-zero total energy detuning and a degenerate incident energy of photons in Figs.3(d),(e),(f) and Figs.4(d),(e),(f). The overall features of two reflected and two transmitted photons are qualitatively similar for a single and two emitters at $\delta E \neq 0$ and $\Delta = 0$ except that there are more oscillations for two emitters. But the value of $|g_{11}(x_1,x_2)|^2$ at $x = 0$ in Fig.3(e) for two emitters is higher compared to a single emitter. It signals a higher photon-photon correlations for two emitters than for a single emitter at a detuned total energy. Physically two emitters able

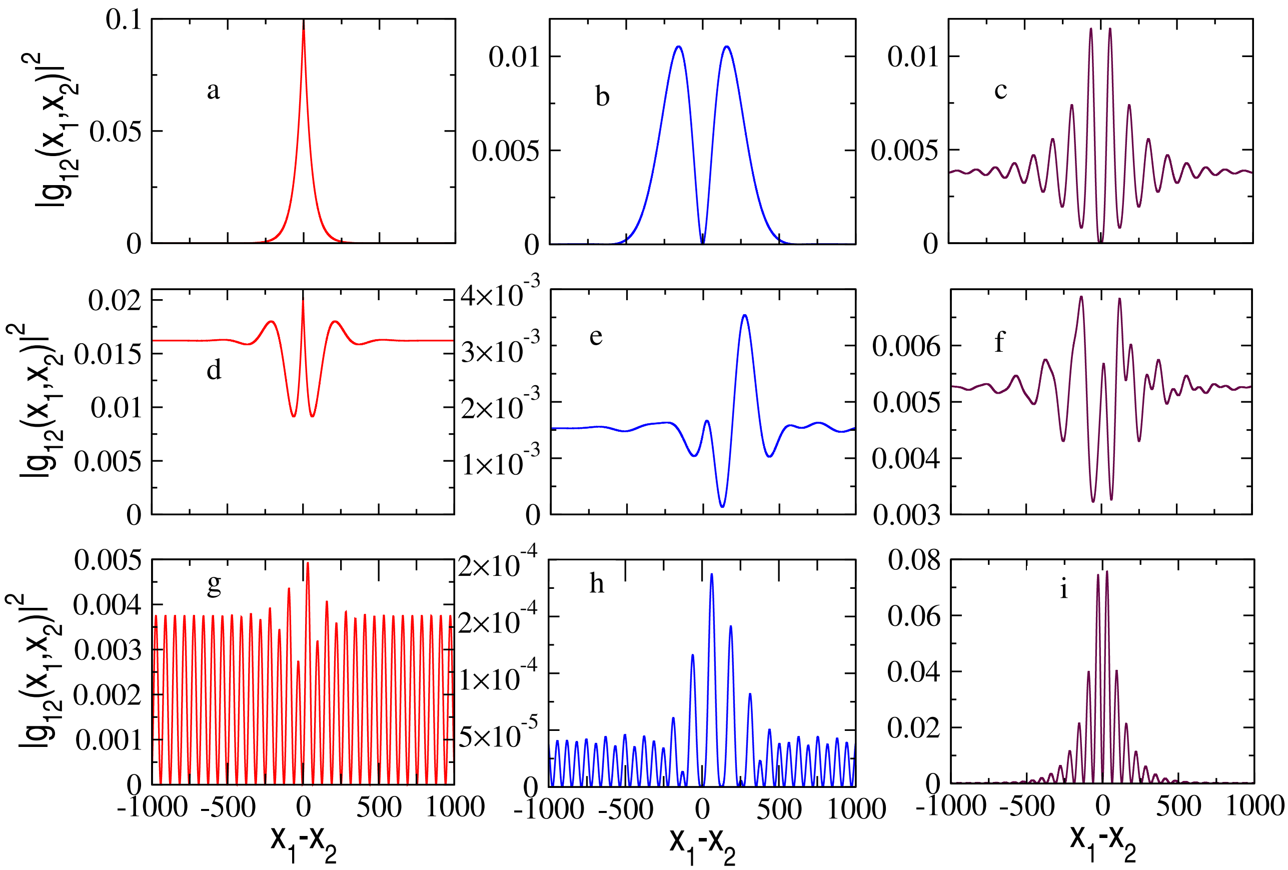

FIG. 5. One reflected and one transmitted photons wave-function $|g_{12}(x_1,x_2)|^2$ for one emitter (first column) and two emitters (middle and last columns) at various incident photon-pair energy detuning δE and energy difference Δ. We use $\Omega_1 = \Omega_2 = \Omega$ and $\Gamma_1 = \Gamma_2 = \Gamma$ in all plots for two emitters. The parameters are, (I) Top row: $\delta E = \Delta = 0,\ E_{k_1} = E_{k_2} = \Omega = 0.35,\ \Gamma = 0.01$, (II) Middle row: $\delta E = 0.04,\ \Delta = 0,\ E_{k_1} = E_{k_2} = 0.35,\ \Omega = 0.33,\ \Gamma = 0.01$, and (III) Bottom row: $\delta E = 0,\ \Delta = -0.1,\ E_{k_1} = 0.3,\ E_{k_2} = 0.4,\ \Omega = 0.35,\ \Gamma = 0.01$. The coupling $J = 0.005$ for the middle column and $J = 0.05$ for the last column.

to reflect photons more than a single emitter away from single photon resonance. We show the role of an energy difference of two incident photons on behavior of $|g_{11}(x_1,x_2)|^2$ and $|g_{22}(x_1,x_2)|^2$ in Figs.3(g),(h),(i) and Figs.4(g),(h),(i) where δE is kept zero. We find the behavior of $|g_{11}(x_1,x_2)|^2$ for a single and two emitters at $J = 0.005$ (at SPR) is similar, though it has a very different behavior away from SPR for two emitters. While $|g_{11}(x_1,x_2)|^2$ oscillates with x for any value of x for the first case, it decays to zero with increasing x for two emitters away from SPR for $\delta E = 0$ and $\Delta \neq 0$. There is almost no transmission of two photons for $E_{k_1}, E_{k_2} \neq \Omega$ at $J = 0.005$. The strength of instaneous coupling J between emitters completely changes the pattern of two transmitted photons correlation in Figs.5(h),(i). The peak of $|g_{11}(x_1,x_2)|^2$ at $x = 0$ for an increasing Δ with $\delta E = 0$ reduces to zero from its maximum value both for a single and two emitters. Therefore, the correlations of two reflected photons changes from *bunching* to *anti-bunching*, i.e., the emitters can induce an effective spatial attraction or repulsion between two reflected photons [15]. Here we find that we can even alternate the nature of photon-photon interactions of two reflected photons in the two-emitters model by changing the coupling strength between emitters. It can be achieved by tuning the separation between emitters [36, 41]. For all values of δE and Δ, $|g_{22}(x_1,x_2)|^2$=0 at $x = 0$ which indicates that two transmitted photons are always *anti-bunched* at the forward direction for two emitters in a 1D waveguide as they are for a single emitter in 1D. The *anti-bunching* of two transmitted photons in our direct coupled emitters model occurs because two photons can not be emitted simultaneously by the right (second) emitter, and the transmitted photons in the right side of the waveguide are solely due emission from the right emitter. While the nature of $|g_{11}(x_1,x_2)|^2$ and $|g_{12}(x_1,x_2)|^2$ both for a single and two emitters is determined by interference between the incident and the emitted photons, thus they show various nature at $x = 0$ depending on the parameters.

We have shown features of $|g_{12}(x_1;x_2)|^2$ away from SPR in the middle and the last rows of Fig.5. While $|g_{12}(x_1;x_2)|^2$ is symmetric as a function of x at $\delta E \neq 0$ and $\Delta = 0$ for $\Gamma_1 = \Gamma_2$ in case of a single emitter, it is asymmetric as a function of x for two emitters at $\delta E \neq 0$

and $\Delta = 0$. The Fig.5(e) shows that the overall feature of $|g_{12}(x_1;x_2)|^2$ including a dip and a large peak is around $x_1 > x_2$. It indicates that reflected photon leaves the left emitter earlier than the transmitted photon leaves the right emitter. It is acceptable as the transmitted photon has to pass two emitters in the two-emitters model. We find $|g_{12}(x_1;x_2)|^2$ is asymmetric as a function of x for both a single and two emitters at SPR when $\delta E = 0$ and $\Delta \neq 0$. In both cases a peak appears at $x_1 > x_2$ which again indicates that the reflected photon leaves the emitters before the transmitted photon at these parameter sets. We also find that the oscillations of $|g_{12}(x_1;x_2)|^2$ at large x for a single emitter disappear for two emitters when $J = 0.05$. Finally we show how stronger correlation

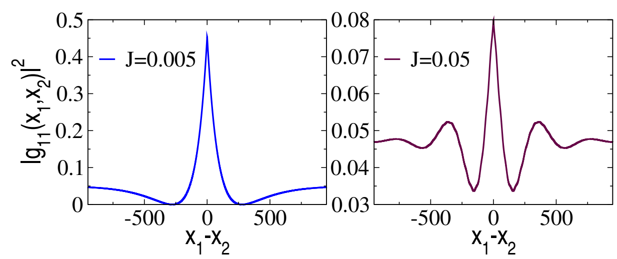

FIG. 6. Two reflected photons wave-function $|g_{11}(x_1,x_2)|^2$ for two emitters at $\delta E = -0.15$, $\Delta = 0$, $E_{k_1} = E_{k_2} = \Omega_1 = 0.35$, $\Omega_2 = 0.5$, $\Gamma_1 = \Gamma_2 = 0.01$.

between photons can be generated by cascaded optical nonlinearity of emitters when $\Omega_1 \neq \Omega_2$. The correlation between the two reflected photons for a degenerate incident energy, i.e., $\Delta = 0$ at $J = 0.005$ and $J = 0.05$ are plotted in Fig.6. We notice $|g_{11}(x_1, x_2 = x_1)|^2 = 0.454$ at $J = 0.005$ is much larger than the maximum correlation $|g_{11}(x_1, x_2 = x_1)|^2 = 1/(2\pi^2)$ for a single emitter in a 1D waveguide.

C. Nonreciprocal photon transmission

We define a photon current operator, $I = i[\mathcal{H}, N_1 - N_2]/2$ where N_1 (N_2) is the total number of photons operator in the left (right) side of the emitter chain. Therefore, $I = i(V_1 c_1^\dagger(0)\sigma_- - V_2 c_2^\dagger(0)\sigma_- - H.c.)/2$. We take expectation of current operator in the single and the two-photon scattering eigenstates of $\mathcal{H}$ to derive a single and two-photon current. The single-photon current for a photon coming from the left (channel 1) is given by

$$I(1;k) = \langle\psi^1_{\rm out}|I|\psi^1_{\rm out}\rangle = \frac{1}{2\pi}|t^1_k|^2. \tag{2.33}$$

Here we mention that $I(1;k) = I(2;k)$ irrespective of the values of couplings and transition energies, including $V_1 \neq V_2$ and $\Omega_1 \neq \Omega_2$. Next we calculate photon current in the two-photon scattering states $|\psi^2_{\rm out}\rangle$ for both the photons with wave-vectors k_1, k_2 being incident from the left (channel 1). The two-photon current $I(1, k_1, k_2)$ has two parts, one $I_0(k_1, k_2)$ is a contribution of two non-interacting photons, and the other $\delta I(1, k_1, k_2)$ is a change of two-photon current due to photon-photon correlation generated by resonant interactions between emitters and photons. The expression for $\delta I(1, k_1, k_2)$ for general values of Ω_j, Γ_j is quite long, and we have kept it in Appendix A.

$$I(1, k_1, k_2) = I_0(k_1, k_2) + \delta I(1, k_1, k_2), \quad \text{where}$$
$$I_0(k_1, k_2) = \frac{\mathcal{L}}{4\pi^2}(|t^1_{k_1}|^2 + |t^1_{k_2}|^2 + 2|t^1_{k_1}|^2\delta_{k_1,k_2}) \tag{2.34}$$

Here $\mathcal{L}$ denotes length of the 1D waveguide. The contribution in two-photon current from the non-interacting photons increases by a factor of two for two degenerate incident photons. This factor was left out in our previous works [18–20]. We also notice that $\delta I(1, k_1, k_2)$ is one order of magnitude smaller than $I_0(k_1, k_2)$. The non-interacting part of two-photon current is the same for forward and backward current for any value of emitter-photon coupling and transition energy of two emitters. The magnitude of $\delta I(1, k_1, k_2)$ is different for both the photons being incident from the left or the right side of the emitters when either $V_1 \neq V_2$ or $\Omega_1 \neq \Omega_2$ or $V_1 \neq V_2$ and $\Omega_1 \neq \Omega_2$. Instead of calculating forward $I(1, k_1, k_2)$ and backward $I(2, k_1, k_2)$ current separately to check asymmetry of two-photon current, we here demonstrate nonreciprocal optical transmission by interchanging the values of transition energy of two emitters in a calculation for two-photon forward current. For example, we find $\delta I(1, k_1, k_2) = -0.0001$ for $\Omega_1 = 0.5$, $\Omega_2 = 0.3$, and $\delta I(1, k_1, k_2) = -0.10017$ for $\Omega_1 = 0.3$, $\Omega_2 = 0.5$ while $k_1 = k_2 = 0.3$, $\Gamma_1 = \Gamma_2 = 0.01$ for both the cases. Thus we find that the total two-photon current as well as the interaction induced two-photon current change are different for an interchange of transition energy of two emitters keeping all other parameters the same, which is equivalent to say, $|I(1, k_1, k_2)| \neq |I(2, k_1, k_2)|$ for $\Omega_1 \neq \Omega_2$ even when $V_1 = V_2$. Previously we propose a few-photon optical diode [18] for a single emitter where it is essential to have different left and right side emitter-photon coupling to get a nonreciprocal optical transmission via broken spatial inversion symmetry. The desired asymmetry in the emitter-photon coupling for a single emitter fixed at a position for a strong emitter-photon coupling is relatively difficult to achieve than to fix two different emitters in a 1D waveguide. Thus our present proposal is much easier to implement in experiment.

The mechanism behind diode like behavior in the two emitters is a redistribution of energy and momentum of photons after passing through the two emitters. The two-photon bound-state part of the wave-function is responsible for the redistribution. The asymmetry in the transition energies generates an asymmetry in the distribution of energy and momentum (via the two-photon bound state) of the photons coming from the left or the right of the emitters. For example, when two degenerate photons are injected at an incident energy on resonance with the first emitter, the photons can pass through the emitter, and their energy gets redistributed which helps

photons to pass the second emitter which has a different transition energy than the first. But if the first emitter's transition energy is different from the energy of the incident photons, photons can not transmit through the emitter and a redistribution of their energy does not occur. Thus photons can not pass the second emitter in the last case even when its transition energy is the same as incident photon energy. Therefore, we get different contributions in the two-photon current change for the two cases. The multi-photon transport is also correlated in this system and the proposed system also acts as an optical diode for many photons. There are several different proposal for realizing optical diodes using various mechanisms, such as, magneto-optic effect, macroscopic optical nonlinearity, indirect inter-band photonic transitions, opto-acoustic effect [49, 50]. Our proposed optical diode works at low intensity of light in the fully-quantum regime compared to most previous proposals in the classical regime, and may have applications to build quantum logic gates for optical quantum information processing and quantum computation. The practical realization of the optical diode relies on achieving a strong emitter-photon coupling in the waveguide and a difference in the transition energy of the emitters.

III. THREE EMITTERS IN A WAVEGUIDE

In this section we briefly mention the main results of a single and two-photon scattering states for a chain of three identical emitters coupled to free propagating photons in a 1D waveguide. The full Hamiltonian of the emitters-photons system within the rotating-wave approximation is $\mathbf{H} = \mathbf{H}_0 + \mathbf{H}_A + \mathbf{H}_C$ where,

$$\begin{aligned}
\mathbf{H}_0 &= -i \int dx\ [a_1^\dagger(x)\partial_x a_1(x) + a_2^\dagger(x)\partial_x a_2(x)], \\
\mathbf{H}_A &= \sum_{j=1}^{3} \Omega|2\rangle_{jj}\langle 2| + J(\sigma_{1-}\sigma_{2+} + \sigma_{2-}\sigma_{3+} + H.c.), \\
\mathbf{H}_C &= (V\sigma_{1+}a_1(0) + V\sigma_{3+}a_2(0) + H.c.). \qquad (3.1)
\end{aligned}$$

The part of the Hamiltonian $\mathbf{H}_0$, $\mathbf{H}_A$ and $\mathbf{H}_C$ denote respectively the propagating photon modes, the emitters and the emitter-photon coupling. Here Ω is a transition energy of the identical emitters and J is a coupling between emitters. V is a coupling strength of photons with the left and right emitters. $a_1^\dagger(x)$ and $a_2^\dagger(x)$ are creation operators of a photon at the left and the right side of the emitters respectively. $\sigma_{j-} = c_{jg}^\dagger c_{je}$ ($\sigma_{j+} = c_{je}^\dagger c_{jg}$) is again a lowering (raising) ladder operator of the jth emitter where $c_{jg}^\dagger(c_{je}^\dagger)$ is a creation operator of the ground state $|1\rangle_j$ (excited state $|2\rangle_j$) of the jth two-level emitter. In this section, we use bold character for those symbols which also appear before for the two emitters model.

A. Single-photon dynamics

The incident state $|\boldsymbol{\psi}_{\rm in}^1\rangle$ of a photon coming from the left of the emitter, and the single-photon wave-function after scattering $|\boldsymbol{\psi}_{\rm out}^1\rangle$ are

$$\begin{aligned}
|\boldsymbol{\psi}_{\rm in}^1\rangle &= \frac{1}{\sqrt{2\pi}} \int dx\ e^{ikx} a_1^\dagger(x)|0,1,1,1\rangle, \\
|\boldsymbol{\psi}_{\rm out}^1\rangle &= \frac{1}{\sqrt{2\pi}} \int dx \big[(\boldsymbol{\phi}_k^1(x)a_1^\dagger(x) + \boldsymbol{\phi}_k^2(x)a_2^\dagger(x))|0,1,1,1\rangle \\
&\quad + \delta(x)(\mathbf{e}_k^1|0,2,1,1\rangle + \mathbf{e}_k^2|0,1,2,1\rangle + \mathbf{e}_k^3|0,1,1,2\rangle)\big].
\end{aligned}$$

The basis state $|n, l_1, m_2, p_3\rangle$ denotes total n number of photons in the waveguide, the left most emitter (no.1) in l_1 state, the middle emitter (no.2) in m_2 state and the right most emitter (no.3) in p_3 state. $\mathbf{e}_k^j$ is an amplitude of the jth excited emitter. The amplitudes of $|\boldsymbol{\psi}_{\rm out}^1\rangle$ are derived by solving five linear coupled (differential) equations obtained from the single-photon Schrödinger equation. The method is similar to the one in Subsec.II A. The amplitudes for an emitter being in the excited state are,

$$\begin{aligned}
\mathbf{e}_k^1 &= \frac{V((E_k - \Omega + i\Gamma/2)(E_k - \Omega) - J^2)}{(E_k - \Omega + i\Gamma/2)^2(E_k - \Omega) - 2J^2(E_k - \Omega + i\Gamma/2)}, \\
\mathbf{e}_k^2 &= \frac{J}{(E_k - \Omega + i\Gamma/2)(E_k - \Omega) - 2J^2}, \\
\mathbf{e}_k^3 &= \frac{J^2 V}{(E_k - \Omega + i\Gamma/2)^2(E_k - \Omega) - 2J^2(E_k - \Omega + i\Gamma/2)}, \qquad (3.2)
\end{aligned}$$

where $\Gamma = V^2$, and the amplitudes of outgoing photon state at the both sides of the waveguide are

$$\begin{aligned}
\boldsymbol{\phi}_k^1(x) &= e^{ikx}\ \theta(-x) + \mathbf{r}_k^1 e^{ikx}\ \theta(x), \\
\boldsymbol{\phi}_k^2(x) &= \mathbf{t}_k^1 e^{ikx}\theta(x), \qquad (3.3)
\end{aligned}$$

where the single-photon transmission and reflection amplitudes are respectively $\mathbf{t}_k^1 = -iV\mathbf{e}_k^3$ and $\mathbf{r}_k^1 = 1 - iV\mathbf{e}_k^1$. The transmission coefficient becomes one at $E_k = \Omega$, and

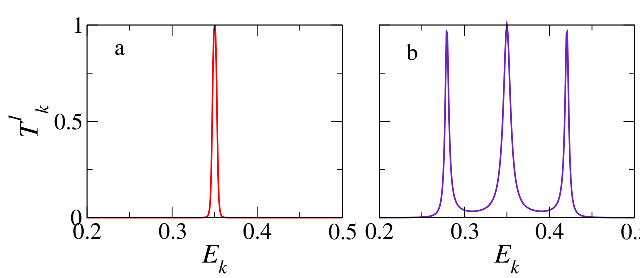

FIG. 7. Single photon transmission T_k^1 through three identical emitters versus energy E_k of an incident photon. In both plots $\Omega = 0.35$, $\Gamma = 0.01$ and (a) $J = 0.0025$, (b) $J = 0.05$.

the corresponding reflection coefficient vanishes. We plot the single-photon transmission coefficient T_k^1 through three identical emitters in Fig.7 for different values of

inter-emitter coupling J. Single peak resonance arises near $E_k = \Omega$ for a very weak coupling between emitters, i.e., $J << \Gamma$ (see Fig.7(a)) while there are three distinct resonant levels for a relatively stronger coupling between emitters.

B. Two-photon dynamics

We again consider that both the photons are injected from the left side of the emitters. The two-photon incoming state is given by,

$$|\boldsymbol{\psi}^2_{\rm in}\rangle = \int dx_1 dx_2 \phi_{\mathbf{k}}(x_1,x_2)\frac{1}{\sqrt{2}}a_1^\dagger(x_1)a_1^\dagger(x_2)|0,1,1,1\rangle \tag{3.4}$$

where $\phi_{\mathbf{k}}(x_1,x_2) = (e^{ik_1x_1+ik_2x_2} + e^{ik_1x_2+ik_2x_1})/2\pi\sqrt{2}$ with $\mathbf{k}=(k_1,k_2)$ and total energy $E_{\mathbf{k}} = k_1+k_2$. The outgoing two-photon scattering state is

$$\begin{aligned}|\boldsymbol{\psi}^2_{\rm out}\rangle = \int dx_1 dx_2 \Big[&\big\{\mathbf{g}_{11}(x_1,x_2)\frac{1}{\sqrt{2}}a_1^\dagger(x_1)a_1^\dagger(x_2) + (\mathbf{e}_1^1(x_1)\sigma_{1+} + \mathbf{e}_1^2(x_1)\sigma_{2+} + \mathbf{e}_1^3(x_1)\sigma_{3+})\delta(x_2)a_1^\dagger(x_1)\\ &+\delta(x_1)\delta(x_2)(\mathbf{e}_{12}\sigma_{1+}\sigma_{2+} + \mathbf{e}_{13}\sigma_{1+}\sigma_{3+} + \mathbf{e}_{23}\sigma_{2+}\sigma_{3+}\big\} + \big\{\mathbf{g}_{12}(x_1;x_2)a_1^\dagger(x_1)a_2^\dagger(x_2) + (\mathbf{e}_2^1(x_1)\sigma_{1+} + \mathbf{e}_2^2(x_1)\sigma_{2+}\\ &+\mathbf{e}_2^3(x_1)\sigma_{3+})\delta(x_2)a_2^\dagger(x_1)\big\} + \mathbf{g}_{22}(x_1,x_2)\frac{1}{\sqrt{2}}a_2^\dagger(x_1)a_2^\dagger(x_2)\Big]|0,1,1,1\rangle.\end{aligned} \tag{3.5}$$

The character of different amplitudes in $|\boldsymbol{\psi}^2_{\rm out}\rangle$ is evident from their definition. We obtain explicit expressions for these amplitudes by solving twelve linear coupled first-order differential equations derived from the two-photon Schrödinger equation. The procedure is similar to that in Subsec.II B, but now we deal with two identical 3×3 square matrices to find the emitter excitation amplitudes instead of 2×2 square matrices in Subsec.II B. The amplitudes for any two emitters in the excited state are given by

$$\begin{aligned}\mathbf{e}_{23} &= \frac{J\mathbf{e}_{13}}{E_{\mathbf{k}} - 2\Omega + i\Gamma/2},\\ \mathbf{e}_{12} &= \frac{J\mathbf{e}_{13} + V(\mathbf{e}^2_{k_1} + \mathbf{e}^2_{k_1})/2\pi}{E_{\mathbf{k}} - 2\Omega + i\Gamma/2},\\ \mathbf{e}_{13} &= \frac{V}{2\pi}\frac{(\mathbf{e}^3_{k_1} + \mathbf{e}^3_{k_2})(E_{\mathbf{k}} - 2\Omega + i\Gamma/2) + J(\mathbf{e}^2_{k_1} + e^2_{k_2})}{(E_{\mathbf{k}} - 2\Omega + i\Gamma/2)(E_{\mathbf{k}} - 2\Omega + i\Gamma) - 2J^2}.\end{aligned}$$

Next we write the amplitudes of a single excited emitter when one photon (which is either at the incident side or reflected) is at the left side of the emitters.

$$\begin{aligned}\mathbf{e}_1^1(x) &= \theta(x)(-\mathbf{c}_1e^{i\lambda_1 x} + \mathbf{c}_2e^{i\lambda_2 x} + \mathbf{c}_3e^{i\lambda_3 x})\\ &\quad+\frac{1}{2\pi}(\mathbf{e}^1_{k_1}\boldsymbol{\phi}^1_{k_2}(x) + \mathbf{e}^1_{k_2}\boldsymbol{\phi}^1_{k_1}(x)), \end{aligned}\tag{3.6}$$

$$\begin{aligned}\mathbf{e}_1^2(x) &= (\frac{\bar\alpha}{4J} + \frac{i\Gamma}{4J})\mathbf{c}_2e^{i\lambda_2 x} + (-\frac{\bar\alpha}{4J} + \frac{i\Gamma}{4J})\mathbf{c}_3e^{i\lambda_3 x}\big)\theta(x)\\ &\quad+\frac{1}{2\pi}(\mathbf{e}^2_{k_1}\boldsymbol{\phi}^1_{k_2}(x) + \mathbf{e}^2_{k_2}\boldsymbol{\phi}^1_{k_1}(x)), \end{aligned}\tag{3.7}$$

$$\begin{aligned}\mathbf{e}_1^3(x) &= \theta(x)(\mathbf{c}_1e^{i\lambda_1 x} + \mathbf{c}_2e^{i\lambda_2 x} + \mathbf{c}_3e^{i\lambda_3 x})\\ &\quad+\frac{1}{2\pi}(\mathbf{e}^3_{k_1}\boldsymbol{\phi}^1_{k_2}(x) + \mathbf{e}^3_{k_2}\boldsymbol{\phi}^1_{k_1}(x)), \end{aligned}\tag{3.8}$$

where $\bar\alpha = \sqrt{32J^2 - \Gamma^2}$, $\lambda_1 = E_{\mathbf{k}} - \Omega + \frac{i\Gamma}{2}$, $\lambda_2 = E_{\mathbf{k}} - \Omega + i\Gamma/4 - \bar\alpha/4$, $\lambda_3 = E_{\mathbf{k}} - \Omega + i\Gamma/4 + \bar\alpha/4$. The constants $\mathbf{c}_j$ in the above relations are arising from the discontinuity of the amplitudes at $x=0$ due to emitter-photon resonant interactions, and they are,

$$\begin{aligned}\mathbf{c}_1 &= \frac{-iV\mathbf{e}_{13}}{2} - \frac{1}{4\pi}((1-\mathbf{r}^1_{k_1})\boldsymbol{\varepsilon}_{k_2} + (1-\mathbf{r}^1_{k_2})\boldsymbol{\varepsilon}_{k_1}),\\ \mathbf{c}_2 &= -\frac{2iJV\mathbf{e}_{12}}{\bar\alpha} - i(\frac{1}{4} - \frac{i\Gamma}{4\alpha})V\mathbf{e}_{13} + \frac{1}{2\pi}(\frac{1}{4} - \frac{i\Gamma}{4\bar\alpha})((1-\mathbf{r}^1_{k_1})\boldsymbol{\varsigma}_{k_2} + (1-\mathbf{r}^1_{k_2})\boldsymbol{\varsigma}_{k_1}),\\ \mathbf{c}_3 &= \frac{2iJVe_{12}}{\bar\alpha} - i(\frac{1}{4} + \frac{i\Gamma}{4\bar\alpha})V\mathbf{e}_{13} + \frac{1}{2\pi}(\frac{1}{4} + \frac{i\Gamma}{4\bar\alpha})((1-\mathbf{r}^1_{k_1})\boldsymbol{\varphi}_{k_2} + (1-\mathbf{r}^1_{k_2})\boldsymbol{\varphi}_{k_1}),\end{aligned}$$

where $\boldsymbol{\varepsilon}_k = V/(k-\Omega+i\Gamma/2)$, $\boldsymbol{\varsigma}_k = V/(k-\Omega+i\Gamma/4-\bar\alpha/4)$, $\boldsymbol{\varphi}_k = V/(k-\Omega+i\Gamma/4+\bar\alpha/4)$. The amplitudes of a single excited emitter when there is one transmitted photon at the right side of the emitters are

$$\mathbf{e}_2^1(x) = \theta(x)(-\tilde{\mathbf{c}}_1 e^{i\lambda_1 x} + \tilde{\mathbf{c}}_2 e^{i\lambda_2 x} + \tilde{\mathbf{c}}_3 e^{i\lambda_3 x}) + \frac{1}{2\pi}(\mathbf{e}^1_{k_1}\boldsymbol{\phi}^2_{k_2}(x) + \mathbf{e}^1_{k_2}\boldsymbol{\phi}^2_{k_1}(x)), \tag{3.9}$$

$$\mathbf{e}_2^2(x) = (\frac{\bar{\alpha}}{4J} + \frac{i\Gamma}{4J})\tilde{\mathbf{c}}_2 e^{i\lambda_2 x} + (-\frac{\bar{\alpha}}{4J} + \frac{i\Gamma}{4J})\tilde{\mathbf{c}}_3 e^{i\lambda_3 x})\theta(x) + \frac{1}{2\pi}(\mathbf{e}^2_{k_1}\boldsymbol{\phi}^2_{k_2}(x) + \mathbf{e}^2_{k_2}\boldsymbol{\phi}^2_{k_1}(x)), \tag{3.10}$$

$$\mathbf{e}_2^3(x) = \theta(x)(\tilde{\mathbf{c}}_1 e^{i\lambda_1 x} + \tilde{\mathbf{c}}_2 e^{i\lambda_2 x} + \tilde{\mathbf{c}}_3 e^{i\lambda_3 x}) + \frac{1}{2\pi}(\mathbf{e}^3_{k_1}\boldsymbol{\phi}^2_{k_2}(x) + \mathbf{e}^3_{k_2}\boldsymbol{\phi}^2_{k_1}(x)), \quad \text{where} \tag{3.11}$$

$$\begin{aligned}
\tilde{\mathbf{c}}_1 &= \frac{1}{4\pi}(\mathbf{t}^1_{k_1}\boldsymbol{\varepsilon}_{k_2} + \mathbf{t}^1_{k_2}\boldsymbol{\varepsilon}_{k_1}) + \frac{iV\mathbf{e}_{13}}{2},\\
\tilde{\mathbf{c}}_2 &= -\frac{1}{2\pi}(\frac{1}{4} - \frac{i\Gamma}{4\bar{\alpha}})(\mathbf{t}^1_{k_1}\boldsymbol{\varsigma}_{k_2} + \mathbf{t}^1_{k_2}\boldsymbol{\varsigma}_{k_1}) - i(\frac{1}{4} - \frac{i\Gamma}{4\bar{\alpha}})V\mathbf{e}_{13} - i\frac{2J}{\bar{\alpha}}V\mathbf{e}_{23},\\
\tilde{\mathbf{c}}_3 &= -\frac{1}{2\pi}(\frac{1}{4} + \frac{i\Gamma}{4\bar{\alpha}})(\mathbf{t}^1_{k_1}\boldsymbol{\varphi}_{k_2} + \mathbf{t}^1_{k_2}\boldsymbol{\varphi}_{k_1}) - i(\frac{1}{4} + \frac{i\Gamma}{4\alpha})V\mathbf{e}_{13} + i\frac{2J}{\bar{\alpha}}V\mathbf{e}_{23}.
\end{aligned}$$

All the terms with $\mathbf{c}_i$ and $\tilde{\mathbf{c}}_i$ in the expressions of the excited emitters in Eqs.3.6-3.11 are contributions from the two-photon bound state which is the source of background fluorescence in the system. Again we define a central of motion coordinate $x_c = (x_1 + x_2)/2$ and a relative motion coordinate $x = (x_1 - x_2)$ of photons. The amplitudes of two photons at different sides of the emitters are

$$\begin{aligned}
\mathbf{g}_{11}(x_1,x_2) = {}& \frac{1}{2\pi\sqrt{2}}(\boldsymbol{\phi}^1_{k_1}(x_1)\boldsymbol{\phi}^1_{k_2}(x_2) + \boldsymbol{\phi}^1_{k_2}(x_1)\boldsymbol{\phi}^1_{k_1}(x_2)) - \frac{iV}{\sqrt{2}}e^{iE_{\mathbf{k}}x_c}(-\mathbf{c}_1 e^{i(\lambda_1 - E_{\mathbf{k}}/2)|x|} + \mathbf{c}_2 e^{i(\lambda_2 - E_{\mathbf{k}}/2)|x|}\\
&+ \mathbf{c}_3 e^{i(\lambda_3 - E_{\mathbf{k}}/2)|x|})\theta(x_1)\theta(x_2), \qquad (3.12)\\
\mathbf{g}_{22}(x_1,x_2) = {}& \frac{1}{2\pi\sqrt{2}}(\boldsymbol{\phi}^2_{k_1}(x_1)\boldsymbol{\phi}^2_{k_2}(x_2) + \boldsymbol{\phi}^2_{k_2}(x_1)\boldsymbol{\phi}^2_{k_1}(x_2)) - \frac{iV}{\sqrt{2}}e^{iE_{\mathbf{k}}x_c}(\tilde{\mathbf{c}}_1 e^{i(\lambda_1 - E_{\mathbf{k}}/2)|x|} + \tilde{\mathbf{c}}_2 e^{i(\lambda_2 - E_{\mathbf{k}}/2)|x|}\\
&+ \tilde{\mathbf{c}}_3 e^{i(\lambda_3 - E_{\mathbf{k}}/2)|x|})\big]\theta(x_1)\theta(x_2), \qquad (3.13)\\
\mathbf{g}_{12}(x_1;x_2) = {}& \frac{1}{2\pi}(\boldsymbol{\phi}^1_{k_1}(x_1)\boldsymbol{\phi}^2_{k_2}(x_2) + \boldsymbol{\phi}^1_{k_2}(x_1)\boldsymbol{\phi}^2_{k_1}(x_2)) - iV\big(-\tilde{\mathbf{c}}_1 e^{i\lambda_1 x_2}e^{i(E_{\mathbf{k}} - \lambda_1)x_1} + \tilde{\mathbf{c}}_2 e^{i\lambda_2 x_2}e^{i(E_{\mathbf{k}} - \lambda_2)x_1}\\
&+ \tilde{\mathbf{c}}_3 e^{i\lambda_3 x_2}e^{i(E_{\mathbf{k}} - \lambda_3)x_1}\big)\theta(x_2 - x_1)\theta(x_1) - iV\big(\mathbf{c}_1 e^{i\lambda_1 x_1}e^{i(E_{\mathbf{k}} - \lambda_1)x_2} + \mathbf{c}_2 e^{i\lambda_2 x_1}e^{i(E_{\mathbf{k}} - \lambda_2)x_2}\\
&+ \mathbf{c}_3 e^{i\lambda_3 x_1}e^{i(E_{\mathbf{k}} - \lambda_3)x_2}\big)\theta(x_1 - x_2)\theta(x_2). \qquad (3.14)
\end{aligned}$$

The first parts of the expressions in Eqs.3.12,3.13,3.14 correspond to two non-interacting photons, while the rest of the terms involving the coefficients $\mathbf{c}_i$ and $\tilde{\mathbf{c}}_i$ are a signature of strong photon-photon correlations. These correlations also represent background fluorescence generated by inelastic scattering of a photon. We show these wave-functions in Figs.8,9 for different values of a total energy detuning $\delta E \equiv E_{\mathbf{k}} - 2\Omega$ and an energy difference $\Delta \equiv E_{k_1} - E_{k_2}$. First, we plot $|\mathbf{g}_{11}(x_1,x_2)|^2$, $|\mathbf{g}_{22}(x_1,x_2)|^2$ and $|\mathbf{g}_{12}(x_1;x_2)|^2$ at single photon resonance, $E_{k_1} = E_{k_2} = \Omega$ in the first column of Fig.8 for $\delta E = \Delta = 0$ and $J = 0.005$. While $|\mathbf{g}_{11}(x_1,x_2)|^2$, $|\mathbf{g}_{22}(x_1,x_2)|^2$ are symmetric as a function of x, $|\mathbf{g}_{12}(x_1;x_2)|^2$ is always asymmetric including the single photon resonance. This is different from the single and the two emitters models. The peak in $|\mathbf{g}_{12}(x_1;x_2)|^2$ for $J = 0.005$ occurs at $x_1 > x_2$ which indicates that the reflected photon leaves the first emitter before the emission of the transmitted photon from the right most emitter. The two transmitted photons are always *anti-bunched* for the three emitters for a same reason as stated for the two emitters. Notice that $|\mathbf{g}_{11}(x_1,x_2 = x_1)|^2 = 1/2\pi^2$ at single photon resonance; this is similar to the single and the two emitters case. But now the form and magnitude of $|\mathbf{g}_{11}(x_1,x_2 = x_1)|^2$, $|\mathbf{g}_{22}(x_1,x_2)|^2$ for the three emitters are quite different from the single and the two emitters at single photon resonance. In fact we find a large magnitude for the peaks of $|\mathbf{g}_{11}(x_1,x_2)|^2$, $|\mathbf{g}_{22}(x_1,x_2)|^2$ and $|\mathbf{g}_{12}(x_1;x_2)|^2$ at non-zero x. Next we show these wave-functions for a detuning of either δE or Δ in the second and third columns of Fig.8. We examine that any detuning reduces the height of the peaks of these wave-function by large amount. Finally we show these wave-functions for a stronger emitter-emitter coupling in Fig.9 for $J = 0.05$. An increase in the strength of coupling between the emitters increases the number oscillations in these wave-functions, and simultaneously reduces the height of the peaks. It can be understood from the single-photon transmission curve of the three emitters in Fig.7 which shows that an increase in the

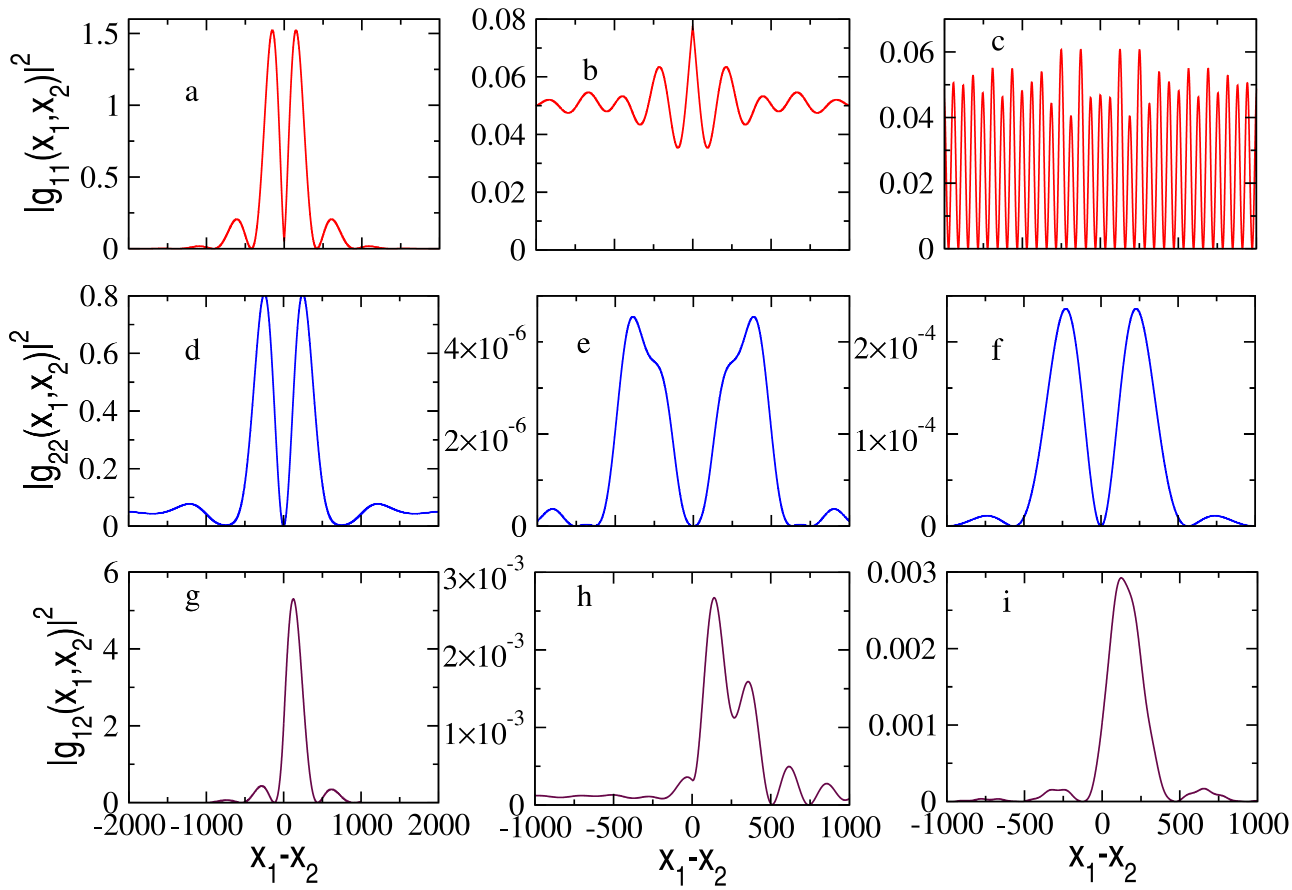

FIG. 8. Two transmitted photons wave-function $|g_{11}(x_1,x_2)|^2$, $|g_{22}(x_1,x_2)|^2$ and $|g_{12}(x_1,x_2)|^2$ for three identical emitters at various incident photon-pair energy detuning δE and energy difference Δ. In all plots $J = 0.005$. The parameters are, (I) First column: $\delta E = \Delta = 0,\ E_{k_1} = E_{k_2} = \Omega = 0.35,\ \Gamma = 0.01$, (II) Middle column: $\delta E = 0.04,\ \Delta = 0,\ E_{k_1} = E_{k_2} = 0.35,\ \Omega = 0.33,\ \Gamma = 0.01$, and (III) Last column: $\delta E = 0,\ \Delta = -0.1,\ E_{k_1} = 0.3,\ E_{k_2} = 0.4,\ \Omega = 0.35,\ \Gamma = 0.01$.

coupling increases the number of peaks in the single photon transmission curve due to the separation of resonant energy levels.

IV. CONCLUSION AND OUTLOOK

In this paper, we calculate an exact solution of the single and two-photon scattering states for free-propagating photons interacting resonantly with two and three two-level emitters in a 1D photonic waveguide. The two-photon transport in these systems are strongly correlated because the two-level emitter can absorb only a single photon at a given time. We derive the single and two-photon transmission in the waveguide for two emitters, and show that the two-photon transmission is nonreciprocal when the two emitters have different transition energies. Recently a large optical non-reciprocity is observed within telecommunication wavelengths in an experiment based on strong optical nonlinearity in two high-quality factor silicon micro-rings [50]. In our proposal we replace those micro-rings by two-level emitters, and employ a strong optical nonlinearity due to emitter-photon interaction in a confined geometry along with an inherent breaking of spatial inversion symmetry by the emitters with different transition energies. We expect that the proposed optical-diode for two different emitters can be realized easily using present experimental techniques. We have also studied how photon-photon correlations scale with an increasing number of emitters in the waveguide. Thus, our study provides a better understanding to control coherent optical nonlinearity in small nanostructures.

Here we generalize a recently developed fully quantum-mechanical transport approach for a single emitter to multiple emitters. The main feature of the approach is a proper inclusion of a two-photon bound state which represents background fluorescence due to inelastic scattering. The present generalized approach should be useful for a wide class of quantum transport problems in variety of systems including the mixed Bose-Fermi cold gases. Now we briefly list some areas where the method can be useful or further developed. First, the above approach should be generalized further for three or more

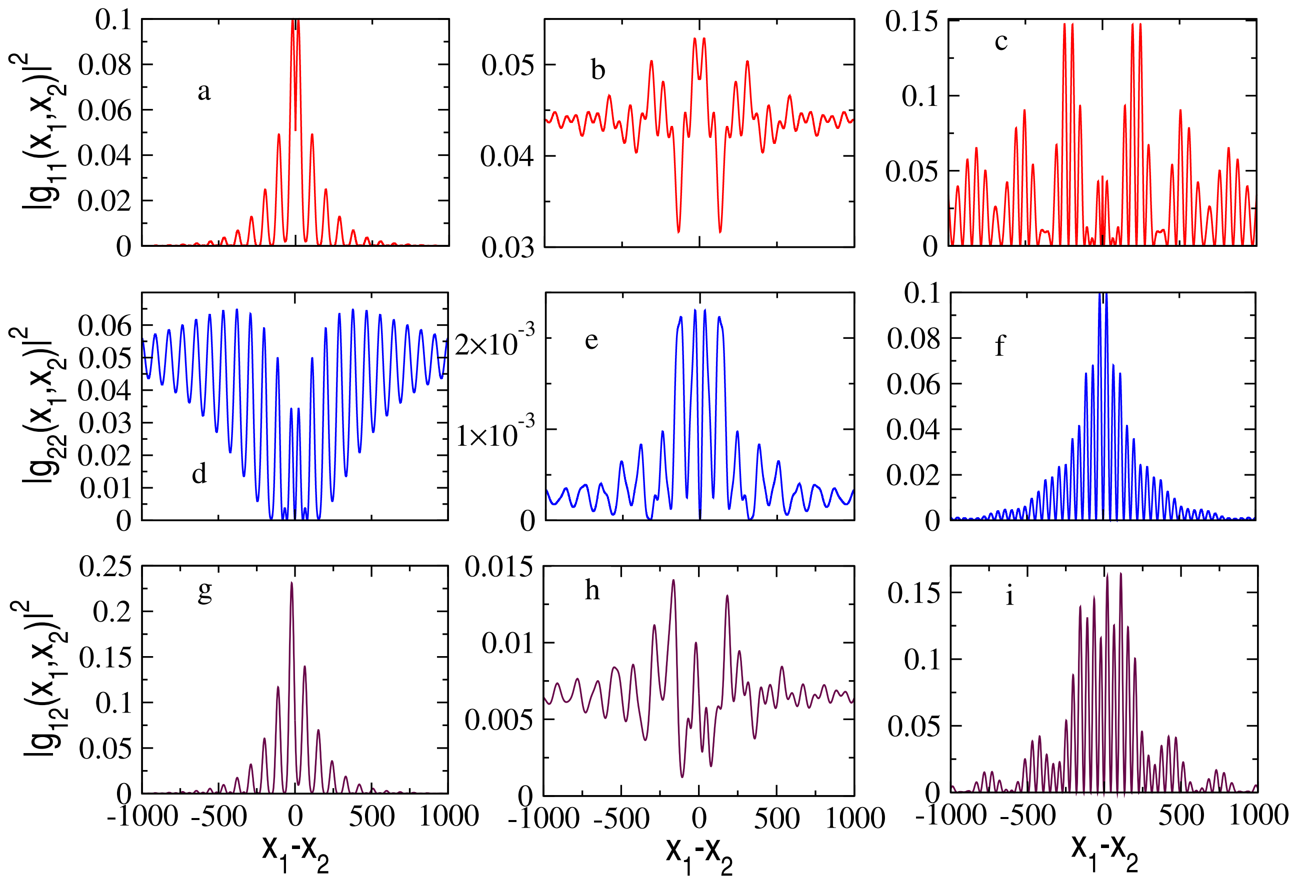

FIG. 9. Two transmitted photons wave-function $|g_{11}(x_1, x_2)|^2$, $|g_{22}(x_1, x_2)|^2$ and $|g_{12}(x_1, x_2)|^2$ for three identical emitters at various incident photon-pair energy detuning δE and energy difference Δ. In all plots $J = 0.05$. The parameters are, (I) First column: $\delta E = \Delta = 0,\ E_{k_1} = E_{k_2} = \Omega = 0.35,\ \Gamma = 0.01$, (II) Middle column: $\delta E = 0.04,\ \Delta = 0,\ E_{k_1} = E_{k_2} = 0.35,\ \Omega = 0.33,\ \Gamma = 0.01$, and (III) Last column: $\delta E = 0,\ \Delta = -0.1,\ E_{k_1} = 0.3,\ E_{k_2} = 0.4,\ \Omega = 0.35,\ \Gamma = 0.01$.

photons. It has been already shown that the open-Bethe ansatz procedure works for multi-particle quantum transport with a single impurity [51]. It would be possible to go beyond single impurity for multi-photon case following the generalized method of this paper. Second, it is also interesting to study the photon-photon correlations mediated by resonant interactions of photons with three or multi-level emitters. Recently, a scaling of electromagnetically induced transparency for weak light field with an increasing number of three-level emitters has been demonstrated in a beautiful experiment [10]. We can employ the technique of the present paper to study these on-going quantum optics experiments [52]. Third, it is equally relevant to have a general routine scheme of correlated two-photon transport for an arbitrary number of emitters in 1D. Fourth, one should also consider two or more channels of emitters in a quasi-1D geometry, and the resonant interactions of emitters between intra and inter channels. The first step in this direction is to evaluate scattering states for two parallel emitters which are both coupled to the propagating photon modes at the both sides of the emitters [52]. Fifth, numerical studies, such as using DMRG [22] or lattice Green's function [53] for discrete photonic lattices with finite band-edges should be extended for multi emitters, and a comparison of these numerical results with the exact results in continuum should be carried out [20]. Finally, progress in the above directions will enrich us enough to study non-equilibrium quantum phase transition of light in the multi-particle emitter-photon systems in comparison with the proposed equilibrium quantum-phase transition of light [54].

V. ACKNOWLEDGMENTS

The author would like to thank H. U. Baranger for sending him their interesting preprint [55] on this subject. The support of the U.S. Department of Energy through LANL/LDRD Program for part of this work is gratefully acknowledged.

Appendix A: Photon-photon interaction induced two-photon current change for two emitters

$$
\begin{aligned}
\delta I(1,k_1,k_2) = {} & \frac{iV_1}{\sqrt{2}}\Big[\frac{\beta^*}{8\sqrt{2}\pi J}(\frac{1}{2}-\frac{\alpha^*}{2\beta^*})c_1^*(e^1_{k_1}r^1_{k_2}\varepsilon^*_{k_1}+e^1_{k_2}r^1_{k_1}\varepsilon^*_{k_2})-\frac{\beta^*}{8\sqrt{2}\pi J}(\frac{1}{2}+\frac{\alpha^*}{2\beta^*})c_2^*(e^1_{k_1}r^1_{k_2}\varsigma^*_{k_1}+e^1_{k_2}r^1_{k_1}\varsigma^*_{k_2}) \\
& +\frac{i\beta c_1}{4\sqrt{2}\pi JV_1}(\frac{1}{2}-\frac{\alpha}{2\beta})(r^{1*}_{k_1}\phi^{1*}_{k_2}(0)\varepsilon_{k_2}+r^{1*}_{k_2}\phi^{1*}_{k_1}(0)\varepsilon_{k_1})-\frac{i\beta c_2}{4\sqrt{2}\pi JV_1}(\frac{1}{2}+\frac{\alpha}{2\beta})(r^{1*}_{k_1}\phi^{1*}_{k_2}(0)\varsigma_{k_2}+r^{1*}_{k_2}\phi^{1*}_{k_1}(0)\varsigma_{k_1}) \\
& -\frac{V_1|\beta|^2}{8\sqrt{2}J^2}|c_1|^2|\frac{1}{2}-\frac{\alpha}{2\beta}|^2\frac{1}{\lambda_--\lambda_-^*}-\frac{V_1|\beta|^2}{8\sqrt{2}J^2}|c_2|^2|\frac{1}{2}+\frac{\alpha}{2\beta}|^2\frac{1}{\lambda_+-\lambda_+^*}+\frac{V_1|\beta|^2}{8\sqrt{2}J^2}c_1c_2^*(\frac{1}{2}+\frac{\alpha^*}{2\beta^*})(\frac{1}{2}-\frac{\alpha}{2\beta})\frac{1}{\lambda_--\lambda_+^*} \\
& +\frac{V_1|\beta|^2}{8\sqrt{2}J^2}c_1^*c_2(\frac{1}{2}-\frac{\alpha^*}{2\beta^*})(\frac{1}{2}+\frac{\alpha}{2\beta})\frac{1}{\lambda_+-\lambda_-^*}\Big]+\frac{iV_1}{2}e_1^{2*}(0)e_{12}+\frac{iV_1}{2}\Big[\frac{i\beta\tilde{c}_1}{4\pi JV_1}(\frac{1}{2}-\frac{\alpha}{2\beta})(\phi^{1*}_{k_1}(0)t^{1*}_{k_2}\varepsilon_{k_1}+\phi^{1*}_{k_2}(0)t^{1*}_{k_1}\varepsilon_{k_2}) \\
& -\frac{i\beta\tilde{c}_2}{4\pi JV_1}(\frac{1}{2}+\frac{\alpha}{2\beta})(\phi^{1*}_{k_1}(0)t^{1*}_{k_2}\varsigma_{k_1}+\phi^{1*}_{k_2}(0)t^{1*}_{k_1}\varsigma_{k_2})-\frac{V_1|\beta\tilde{c}_1|^2}{8J^2}|\frac{1}{2}-\frac{\alpha}{2\beta}|^2\frac{1}{\lambda_--\lambda_-^*}-\frac{V_1|\beta\tilde{c}_2|^2}{8J^2}|\frac{1}{2}+\frac{\alpha}{2\beta}|^2\frac{1}{\lambda_+-\lambda_+^*} \\
& +\frac{V_1|\beta|^2}{8J^2}\tilde{c}_1^*\tilde{c}_2(\frac{1}{2}-\frac{\alpha^*}{2\beta^*})(\frac{1}{2}+\frac{\alpha}{2\beta})\frac{1}{\lambda_+-\lambda_-^*}+\frac{V_1|\beta|^2}{8J^2}\tilde{c}_1\tilde{c}_2^*(\frac{1}{2}+\frac{\alpha^*}{2\beta^*})(\frac{1}{2}-\frac{\alpha}{2\beta})\frac{1}{\lambda_--\lambda_+^*} \\
& +\frac{\beta^*}{8\pi J}\tilde{c}_1^*(\frac{1}{2}-\frac{\alpha^*}{2\beta^*})(e^1_{k_1}t^1_{k_2}\varepsilon^*_{k_1}+e^1_{k_2}t^1_{k_1}\varepsilon^*_{k_2})-\frac{\beta^*}{8\pi J}\tilde{c}_2^*(\frac{1}{2}+\frac{\alpha^*}{2\beta^*})(e^1_{k_1}t^1_{k_2}\varsigma^*_{k_1}+e^1_{k_2}t^1_{k_1}\varsigma^*_{k_2})\Big]-\frac{i}{2}\Big[-\frac{V_2^2}{2}\Big(\frac{|c_2|^2+|\tilde{c}_2|^2}{\lambda_+-\lambda_+^*} \\
& +\frac{|c_1|^2+|\tilde{c}_1|^2}{\lambda_--\lambda_-^*}+\frac{c_1c_2^*+\tilde{c}_1\tilde{c}_2^*}{\lambda_--\lambda_+^*}+\frac{c_1^*c_2+\tilde{c}_1^*\tilde{c}_2}{\lambda_+-\lambda_-^*}\Big)+\frac{V_2^2}{4\pi V_1}(c_1^*r^1_{k_1}e^2_{k_2}\varepsilon^*_{k_2}+c_1^*r^1_{k_2}e^2_{k_1}\varepsilon^*_{k_1}+c_2^*r^1_{k_1}e^2_{k_2}\varsigma^*_{k_2}+c_2^*r^1_{k_2}e^2_{k_1}\varsigma^*_{k_1}) \\
& +\frac{iV_2}{4\pi V_1}(c_1r^{1*}_{k_1}t^{1*}_{k_2}\varepsilon_{k_2}+c_1r^{1*}_{k_2}t^{1*}_{k_1}\varepsilon_{k_1}+c_2r^{1*}_{k_1}t^{1*}_{k_2}\varsigma_{k_2}+c_2r^{1*}_{k_2}t^{1*}_{k_1}\varsigma_{k_1})\Big]-\frac{iV_2}{2}e_2^{1*}(0)e_{12}-\frac{iV_2}{8\pi V_1}\Big[it^{1*}_{k_1}t^{1*}_{k_2}(\tilde{c}_1(\varepsilon_{k_2}+\varepsilon_{k_2}) \\
& +\tilde{c}_2(\varsigma_{k_2}+\varsigma_{k_2}))+V_2(\tilde{c}_1^*e^2_{k_1}t^1_{k_2}\varepsilon^*_{k_1}+\tilde{c}_1^*e^2_{k_2}t^1_{k_1}\varepsilon^*_{k_2}+\tilde{c}_2^*e^2_{k_1}t^1_{k_2}\varsigma^*_{k_1}+\tilde{c}_2^*e^2_{k_2}t^1_{k_1}\varsigma^*_{k_2})\Big].
\end{aligned} \tag{A1}
$$

[1] Q. A. Turchette, C. J. Hood, W. Lange, H. Mabuchi and H. J. Kimble, Phys. Rev. Lett. **75**, 4710 (1995).
[2] A. Imamoglu, H. Schmidt, G. Woods and M. Deutcsh, Phys. Rev. Lett. **79**, 1467 (1997).
[3] S. E. Harris and Y. Yamamoto, Phys. Rev. Lett. **81**, 3611 (1998).
[4] K. M. Birnbaum *et al.*, Nature **436**, 87 (2005).
[5] I. Schuster,*et al.* Nature Phys. **4**, 382 (2008).
[6] B. Dayan et. al., Science **319**, 1062 (2008).
[7] K. Srinivasan and O. Painter, Nature **450**, 862 (2007).
[8] G. Zumofen, N. M. Mojarad, V. Sandoghdar and M. Agio, Phys. Rev. Lett. **101**, 180404 (2008).
[9] J. Hwang, M. Pototschnig, R. Lettow, G. Zumofen, A. Renn, S. Götzinger and V. Sandoghdar, Nature **460**, 76 (2009).
[10] M. Mücke et. al., Nature **465**, 755 (2010).
[11] O. Astafiev, A. M. Zagoskin, A. A. Abdumalikov Jr., Yu. A. Pashkin, T. Yamamoto, K. Inomata, Y. Nakamura and J. S. Tsai, Science **327**, 840 (2010).
[12] A. Ourjoumtsev, A. Kubane, M. Koch, C. Sames, P. W. H. Pinske, G. Rempe and K. Murr, Nature **474**, 623 (2011).
[13] A. Reinhard, T. Volz, M. Winger, A. Badolato, K. J. Hennessy, E. L. Hur and A. Imamoglu, Nature Photonics **6**, 93 (2012).
[14] T. Peyronel, O. Firstenberg, Q. Y. Liang, S. Hofferberth, A. V. Gorshkov, T. Pohl, M. D. Lukin and V. Vuletic, Nature **488**, 57 (2012).
[15] J.-T. Shen and S. Fan, Phys. Rev. Lett. **98**, 153003 (2007); Phys. Rev. A **76**, 062709 (2007).
[16] D. E. Chang, A. S. Sorensen, E. A. Demler and M. D. Lukin, Nature Phys. **3**, 807 (2007).
[17] T. Shi and C. P. Sun, Phys. Rev. B **79**, 205111 (2009).
[18] D. Roy, Phys. Rev. B **81**, 155117 (2010).
[19] D. Roy, Phys. Rev. Lett. **106**, 053601 (2011).
[20] D. Roy, Phys. Rev. A **83**, 043823 (2011).
[21] J. Q. Liao and C. K. Law, Phys. Rev. A **82**, 053836 (2010).
[22] P. Longo, P. Schmitteckert and K. Busch, Phys. Rev. Lett.**104**, 023602 (2010).
[23] H. Zheng, D. J. Gauthier and H. U. Baranger, Phys. Rev. Lett. **107**, 223601 (2011).
[24] E. Rephaeli and S. Fan, Phys. Rev. Lett. **108**, 143602 (2012).
[25] A. Faraon et. al., Appl. Phys. Lett. **90**, 073102 (2007); A. Faraon et. al., Optics Exp. **16**, 12154 (2008).
[26] A. V. Akimov et. al., Nature **450**, 402 (2007).
[27] A. Wallraff, D. I. Schuster, A. Blais, L. Frunzio, R.-S. Huang, J. Majer, S. Kumar, S. M. Girvin and R. J. Schoelkopf, Nature **431**, 162 (2004).
[28] E. Vetsch et.al., Phys. Rev. Lett. **104**, 203603 (2010).
[29] J. Claudon et. al., Nat. Photonics **4**, 174 (2010).
[30] T. M. Babinec et. al., Nat. Nanotech. **5**, 195 (2010).

[31] I. Gerhardt, G. Wrigge, P. Bushev, G. Zumofen, M. Agio, R. Pfab and V. Sandoghdar, Phys. Rev. Lett.**98**, 033601 (2007).
[32] G. Hetet, L. Slodicka, M. Hennrich and R. Blatt, Phys. Rev. Lett.**107**, 133002 (2011).
[33] F. Diedrich and H. Walther, Phys. Rev. Lett. **58**, 203 (1987).
[34] W. M. Itano, J. C. Bergquist and D. J. Wineland, Phys. Rev. A **38**, 559 (1988).
[35] G. S. Agarwal, A. C. Brown, L. M. Narducci and G. Verti, Phys. Rev. A **15**, 1613 (1977).
[36] Z. Ficek, R. Tanas and S. Kielich, Opt. Acta **30**, 713 (1983).
[37] T. Richter, Opt. Commun. **80**, 285 (1991).
[38] C. Skornia, J. von Zanthier, G. S. Agarwal, E. Werner and H. Walther, Phys. Rev. A **64**, 063801 (2001).
[39] R. DeVoe and R. Brewer, Phys. Rev. Lett. **76**, 2049 (1996).
[40] T. Rudolph, Z. Ficek and B. Dalton, Phys. Rev. A **52**, 636 (1995).
[41] A. Beige and G. Hegerfeldt, Phys. Rev. A **58**, 4133 (1998); **59**, 2385 (1999).
[42] Z. Ficek and B. C. Sanders, Phys. Rev. A **41**, 359 (1990).
[43] H. J. Carmichael, *An Open Systems Approach to Quantum Optics* (Lecture Notes in Physics) (Berlin: Springer).
[44] D. Witthaut and A. S. Sorensen, New J. Phys. **12**, 043052 (2010).
[45] D. Bozyigit et. al., Nature Physics **7**, 154 (2011)
[46] B. R. Mollow, Phys. Rev. **188**, 1969 (1969).
[47] J. T. Hoffges, H. W. Baldauf, T. Eichler, S. R. Helmfrid and H. Walther, Optics Communications **133**, 170 (1997).
[48] D. E. Chang, V. Gritsev, G. Morigi, V. Vuletic, M. D. Lukin and E. A. Demler, Nature Physics **4**, 884 (2008).
[49] M. Scalora *et al.*, J. Appl. Phys. **76**, 2023 (1994); K. Gallo *et al.*, Appl. Phys. Lett. **79**, 314 (2001); S. F. Mingaleev and Y. S. Kivshar, J. Opt. Soc. Am. B **19**, 2241 (2002); J. Hwang *et al.*, Nature Mat. **4**, 383 (2005); Z. Yu and S. Fan, Nat. Photonics **3**, 91 (2009); M. S. Kang, A. Butsch and P. S. J. Russel, Nat. Photonics **5**, 549 (2011) L. Bi *et al.*, Nat. Photonics **5**, 758 (2011).
[50] L. Fan, J. Wang, L. T. Varghese, H. Shen, B. Niu, Y. Xuan, A. M. Weiner and M. Qi, Science **335**, 447 (2012).
[51] A. Nishino, T. Imamura and N. Hatano, Phys. Rev. B **83**, 035306 (2011).
[52] D. Roy, unpublished notes (2012).
[53] A. Dhar, D. Sen and D. Roy, Phys. Rev. Lett. **101**, 066805 (2008); D. Roy, A. Soori, D. Sen and A. Dhar, Phys. Rev. B **80** 075302 (2009); D. Roy, Phys. Rev. B **80**, 245304 (2009).
[54] D. G. Angelakis, M. F. Santos and S. Bose, Phys. Rev. A (Rap. Com.) **76**, 031805 (2007).
[55] H. Zheng and H. U. Baranger, arXiv: 1206.4442 (2012).